Aerodynamic and Structural Analysis of UAV

A Final Year Project Report

Presented to

SCHOOL OF MECHANICAL & MANUFACTURING ENGINEERING

Department of Mechanical Engineering

NUST

ISLAMABAD, PAKISTAN

_____

In Partial Fulfillment

of the Requirements for the Degree of

Bachelor of Mechanical Engineering

_____

By

ZAIN Ul ABIDIN

ABDUL MOEED

ANS AHMAD KHAN

June, 2022
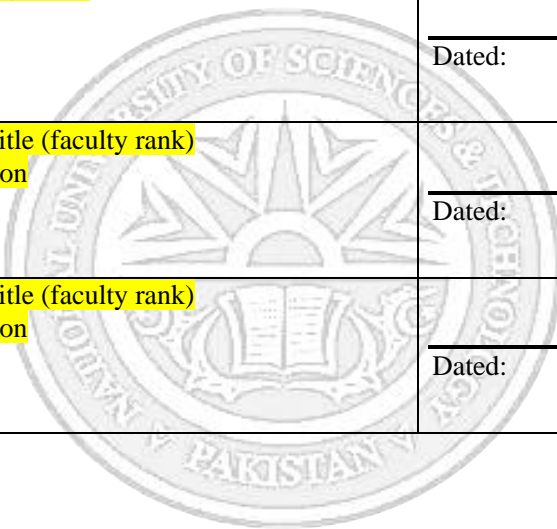
EXAMINATION COMMITTEE

We hereby recommend that the final year project report prepared under our supervision by:

ZAIN UL ABIDIN   245158

ABDUL MOEED   261914

ANS AHMAD KHAN   256410

Titled: "**Aerodynamic and Structural Analysis of UAV**" be accepted in partial fulfillment of the requirements for the award of DEGREE NAME degree with grade ___

Supervisor: Name, Title (faculty rank) Affiliation	_____ Dated:
Committee Member: Name, Title (faculty rank) Affiliation	_____ Dated:
Committee Member: Name, Title (faculty rank) Affiliation	_____ Dated:

ABSTRACT

Unmanned Armed Vehicles (UAVs) are used in surveillance, offensive, and other tactical operations by the military of several countries of the world including Pakistan. This study focuses on the aerodynamics and design of an unmanned aerial vehicle (UAV). Conceptual design, preliminary design, structural analysis, and a computational fluid dynamics simulation of the vehicle are all part of the method. We'll aim to develop a low-cost fixed wing unmanned aerial vehicle (UAV) that can fly independently utilizing low-cost materials. We'll build it with the following design factors in mind: basic airframe configuration, wing configuration, straight wing configuration, and tail configuration. Once we've finalized our design, we'll run a structural analysis on our model to get crucial stress and displacement data. We will highlight the areas where we are getting higher values of stress and huge deformations. We also perform computational fluid dynamics analysis of the model to obtain lift and drag forces along with pressure distribution curve. Using our results, we will perform required changes in our design to make a final design.

ACKNOWLEDGMENTS

ORIGINALITY REPORT

19 docero.tips
    Internet Source   <1%

20 Mohammad H. Sadraey. "Aircraft Design",
    Wiley, 2012   <1%
    Publication

21 Submitted to University of Derby
    Student Paper   <1%

22 Submitted to University Of Tasmania
    Student Paper   <1%

23 epdf.pub
    Internet Source   <1%

24 Submitted to University of Strathclyde
    Student Paper   <1%

25 www.scientific.net
    Internet Source   <1%

26 Submitted to Middle East Technical University
    Student Paper   <1%

27 Submitted to University of Newcastle upon
    Tyne   <1%
    Student Paper

28 Submitted to University of Petroleum and
    Energy Studies   <1%
    Student Paper

29 Submitted to Zewail City of Science and
    Technology   <1%

TABLE OF CONTENTS

LIST OF TABLES

LIST OF FIGURES

ABBREVIATIONS

UAV	Unmanned air vehicle
AoA	Angle of attack
NACA	National Advisory Committee for Aeronautics
FEA	Finite Element Analysis

NOMENCLATURE

F_D	Drag Force
F_L	Lift Force
P	Density
V	Velocity
A	Area
C_d	Drag coefficient
C_{-L}	Lift coefficient
C_{-P}	Coefficient of pressure
M	Meter
Kg	Kilogram
Ft	Feet
m^2	Meter squared

1 CHAPTER 1: INTRODUCTION

1.1   Motivation:

The motivation of selecting this project is to provide an optimum and feasible design of fixed wing Unmanned Aerial Vehicle (UAV) for defense, surveillance, agriculture, network coverage, by performing complete structural and aerodynamic analysis of its airframe.

1.1.1 Military and Defense point of view:

UAVs raises the possibility of conducting military operations in more efficient and less risky fashion as these vehicles are unmanned and can fly autonomously through software based-controlled flight plans working in conjunction with on board sensors and GPS while carrying lethal payload to destroy its target. In this way there is no need for a human pilot on board. It is an industrial project so any research, any advancement that we make, will definitely end up in setting a platform for further progress and evolution of fixed wing UAVs in Pakistan strengthening our defenses.

1.1.2 Agriculture

UAVs can be used to capture the image of farmer's crop with wide variety of cameras filters through which farmers can get better information about crop's health and identify areas of crops that require specific forms of maintenance and attention. Pest activity can be monitored quite easily. Through UAVs, farmers can look for where they require more essential nutrients and water for different crops. Pakistan's economy significantly relies on agriculture industry. Government of Pakistan has approved the use of drone technology for agricultural reasons. Farmers can collect data much faster than the traditional methods. This smart technology reduces time being spent on the field which in turn saves farmers money and labor equipment. UAVs are helpful in land management including drainage issues, yield estimations and soil moisture

1.1.3 Stability

UAVs run on rechargeable batteries rather than gasoline which make these vehicles a sustainable solution. The limitations posed by humans are exterminated through the use of UAVs

making these vehicles more suitable and reliable as compared to manned aerial vehicles. Design process of UAVs usually requires lower factor of safety as compared to that of manned aircraft due to the absence of human life in UAV.

1.1.4 Interest in aerodynamics

Aerodynamics is a very fascinating branch of physics which explains how an airplane flies in air. Although we have not studied any detailed aerodynamic related course in our degree but one of our group members has a strong interest in this field and has completed many aviation related projects in last three years. One member wants to pursue his master's degree in this field. In this way, this project is a golden opportunity for all three of us to explore new areas and recent advancements with ongoing research in this field by working on fixed wing UAV covering all the fluid mechanics and aerodynamics theory aspects in detail.

1.1.5 Aerial Photography and Surveillance

Aerial surveillance is widely used in the public sector as well, especially during disaster management operations. UAV is automatically deployed and landed, and the system analyzes the aerial data, creating best photos and digital elevation models to assist in surveying reports. It can be flown at low altitudes to collect high-resolution data that rivals traditional survey methods. It can be used to track the project milestones as the project progresses and yield aerial images of the end result. In civil engineering, these aerial vehicles are used for feasibility surveys in transportation routes and infrastructure inspection in bridges, cell phone towers, power lines, solar panels.

1.1.6 Inspiration from Glide-bomb (GB-6) China

The project design is inspired from Glide-bomb (GB-6) China which is easy to manufacture and has compact design with high payload capacity. This X-tail configuration has low Radar cross-section (measure of how detectable an object is by radar).

1.2   Problem Statement:

Aerodynamic and Structural Analysis of a UAV

1.3   Objectives:

The objectives of this project are as follows:

•   Designing a 3D CAD model for the UAV

•   Generating a computational mesh for the model

•   Analyzing stresses and deformation by finite element modeling (FEM) analysis using ANSYS, highlighting the areas of very large stresses and deformations.

•   Performing static CFD analysis for aerodynamic loads, computing the Lift and Drag forces along with pressure distribution curve.

•   Further analyzing the structure with aerodynamic forces obtained via CFD.

•   Providing recommendations for improvement.

2 CHAPTER 2: LITERATURE REVIEW

For the design and analysis of fixed Wing UAV, following techniques are used.

1. Design of Fixed wing Unmanned Aerial Vehicle
    a. Feasible and optimum Design Parameters
    b. Airfoil Selection for fixed wing
    c. Weight and CG estimation
    d. Complete design calculation for wing, fuselage and empennage.

2. Structural Analysis
a. Force-Displacement Relationship
b. Bending and Torsion loads
c. Beam Deflection
d. Material selection principles with respect to performance, mechanical properties, and constraints.
e. Boundary conditions for structure
f. Computational meshing of structure
g. Failure of structure under given loads

3. Aerodynamic Analysis

a) Mesh generation
b) Boundary conditions
c) Selection of turbulence model and other parameters
d) Computation of the Lift and Drag forces
e) Pressure distribution curve around the airfoil
f) Optimization of lift-to-drag ratio

Research paper	Abstract
Design of High-Altitude Long Endurance UAV: Structural Analysis of composite wing using Finite Element Method	1st generation if HALE UAVs used Balsa wood for wing structure. Extreme side wing cause large bending to its high aspect ratio results in failure of wings. Designing the 2nd generation of HALE UAV using composite materials instead of balsa wood and compare the results. Finite element analysis is performed using ABAQUS/CAE to predict stress and deformations. Failure criteria like Tsai-Wu and Von-Misses were used to check for structure failure.
Structural Analysis of Fuselage and Empennage of High-Altitude Long Endurance UAV	The fuselage and empennage of the HALE UAV were structurally analyzed in this research paper. Flight load analysis provides critical loading conditions for structural analysis, and the findings of structural sizing for weight reduction are then reported. For a UAV to fly a long period in harsh environment of the stratosphere, it requires high Lift-Drag Ratio and weight reduction of the structure. Critical loads on fuselage and empennage are applied and results are evaluated.
Structural deformation and stress analysis of aircraft Wing by Finite Element Method	The paper outlines the key parameters and variables for designing the wing of aircraft to take the full aircraft weight during flying from conceptual stage to detail design. Structural properties of wing are analyzed by using finite element method. Material is selected with efficient and optimum properties to overcome drag for which responsible properties are displacement and stress. Research on aero-elastic investigation for good aerodynamic design of wing is still going on.
Structural and CFD Analysis of Unmanned Aerial Vehicle by using	The paper focuses on reducing the structural weight and drag of an unmanned aerial vehicle (UAV) while increasing its endurance. The structural strength parameters of UAV frames are studied using Finite Element Analysis to attain a high strength to weight ratio. Using the k-e

COMSOL Multiphysics	turbulence model, a computational fluid dynamic analysis (CFD) is done for various angles of attack and vehicle speeds to estimate the drag coefficient.
Design and Analysis of UAV Fuselage	The UAV in this study is light-weight and designed for short-term use, having a mass carrying capability of 2kg. Initially, the form is taken into account in terms of aerodynamics. The installation of internal systems, cargo location, and fuselage construction are then developed. Under the landing situation of a static model with 3.5g acceleration, finite element analysis is performed for stress analysis. Maximum stress from FEA analysis shows that it is less than the material's strength with Factor of safety of 1.1 (safe design)
Aerodynamic design of a MALE UAV	This paper discusses the aerodynamic design procedure of a Medium-Altitude-Long-Endurance (MALE) UAV. The procedure includes both the conceptual as well as preliminary design phases. Different aspects like the wing design, fuselage design, winglet and empennage design and optimization technique are discussed.
Design, performance evaluation and optimization of a UAV	This paper discusses the design, construction and testing of a small size light UAV. The UAV is being designed to serve as a reconnaissance plane, capable of high-quality photography and video recording. The design phase began with a linear aerodynamic performance and stability analysis. Following that, CFD was used to analyze the aerodynamic properties and efficiency of the airfoil section, the wing, and the entire arrangement. Finally, computer optimization was used to further increase the aerodynamic efficiency of the entire design.
Design of a Low-Cost Fixed Wing UAV	This paper focuses the design, and fabrication of fixed wing UAV. Different characteristics of the UAV include Six parameters of UAV's structure will be optimized based on basic airframe configuration, wing configuration, straight wing, tail configuration, fuselage material, and propeller location.

	The resulted and manufactured prototype of fixed-wing UAV will be tested in autonomous fight tests.
Design of A Medium Range Tactical UAV and Improvement of Its Performance by Using Winglets	This paper focuses the design, performance analysis and aerodynamic improvement of a medium range tactical UAV. Different characteristics of the UAV include; cruising altitude of 3500m, range of 150 km, endurance of approximately 10-12 hours and payload of 60 kg. The aerodynamic improvement process includes an increase in span efficiency through the use and comparison of various wingtip shapes, which leads to an increase in L/D ratio, endurance, climb rate or weight reduction, as well as a decrease in necessary power.
Conceptual Design of an Unmanned Fixed-Wing Aerial Vehicle Based on Alternative Energy	The aerodynamics and design of an unmanned aerial vehicle (UAV) powered by solar cells are the topic of this research. The flying mission in this study begins with the vehicle design attempting to reach maximum altitude; after that, the UAV begins to glide, and battery charge recovery is completed thanks to the solar cells. The aerodynamic study is centered on a UAV as a gliding vehicle, with the calculations beginning with the assessment of weight and aerodynamics and ending with the optimal glide angle at this stage. The aerodynamic study is really obtained for a preliminary design, which includes the UAV's wing, fuselage, and empennage.

Table 1 Research Paper Used

A UAV (Unmanned Aerial Vehicle) is a plane that does not have a human pilot on board. UAV flight can be controlled either by a human operator or by onboard computers with varying degrees of autonomy. A UAV system consists of a UAV, a ground-based controller, and a communication system between the two.

2.1 History

- In 1922, the Aircraft carrier (HMS Argus) launched first unmanned aircraft (RAE 1921 target)

- First successful flight was operated by British RAE 1921 Target 1921 in which radio-controlled unmanned aircraft flew for 39 minutes without human pilot onboard in September 1924.

- In June 1944, German military used unmanned aircraft for combat purposes in the cruise missile role. Similar role was performed by U.S. Navy on 19th October 1944 in the strike role by dropping 10 bombs on Japanese gun positions on Ballale Island.

- Unmanned Aircraft was used for scientific research by the U.S. Weather Bureau to collect meteorological data for the flights in thunderstorms in April 1946.

- In 1955, unmanned aircraft was designed for reconnaissance fielded by the U.S. and British armies.

- The first free flight by an unmanned helicopter was performed by the Gyrodyne QH-50A at Maryland. [1]

2.2 Countries

Two main countries, probably the world leaders, in the development and design of UAV are USA and Israel. The United States classify their main operational UAVs using the RQ abbreviation. Israel Aircraft industry is also producing state of the art UAVs and sell them to the world countries depending on their need. Australian aerospace industry has been designing UAVs since 1950s which has assisted Australian army in coastal watch and surveillance. [1]

2.3 Classification of UAVs by performance characteristics

There are a broad number of performance characteristics upon which UAVs are classified. Weight, endurance, range, speed, wing loading, wingspan, maximum altitude and cost are important specifications that differentiate different types of UAVs and give rise to useful classification systems. Engine type and maximum power developed are the other two parameters based on which UAVs are examined and classified.

2.3.1 Classification by Weight

UAVs ranges from micro-UAVs which weigh only a few pounds right up to colossal Global Hawk (Tier III) which weighs over 11 tonnes. Four classifications can be proposed to distinguish UAVs by take-off weight.

UAVs with large weights require more lift and thrust. Therefore, wingspan area will increase and type of power plant chosen will differ. Electric motors are used in light weight UAVs while super heavy weights need turbo jets or turbo fan engines for their operation.[1]

Below is the table representing the classification of UAVs by Weight:

Designation	Weight Range	Example
Super Heavy	>2000 kg	Global Hawk
Heavy	200-2000 kg	A-160
Medium	50-200 kg	Raven
Light	5-50 kg	RPO Midget
Micro	<5kg	Dragon Eye

Table 2. Classification by Weight

2.3.2 Classification based on Endurance and Range

UAVs can also be classified based on their endurance and range. Both of these factors are linked because the longer a UAV can stay in the air (airborne), the wider its operating radius, or range. When constructing a UAV, these two characteristics must be taken into account to determine how distant the mission goal is from the launch point. The designer also sets how often the UAV must refuel and how much time it must spend in the air to perform its task, as well as how much time it must remain grounded. [1]

Long, medium and short endurance-range classifications of UAVs are presented in the table below with examples:

Category	Endurance	Range	Example
High	>24 hours	>1500 km	Predator B
Medium	5-24 hours	100-400 km	Silver Fox
Low	<5 hours	< 100 km	Pointer

Figure 1 Classification by Endurance and Range

2.3.3 Classification by Maximum Altitude

UAVs can also be classified depending on their operational altitudes or flight ceilings. To avoid being detected and destroyed by the adversary during military operations, UAVs must have limited visibility, which necessitates a high altitude. High-altitude UAVs can complete the duty of imaging and reconnaissance by capturing photographs of the largest possible area of land. [1]

A low, medium and high-altitude classification for UAVs is represented in the table below:

Category	Max. Altitude	Example
Low	<1000 m	Pointer
Medium	1000-10000 m	Finder
High	>1000 m	Darkstar

Figure 2 Classification by Maximum Altitude

2.3.4 Classification by Wing Loading

Another relevant criterion for categorizing UAVs is their wing loading capability. The overall mass of an aircraft (UAV) divided by the area of its wing is referred to as wing loading. The stalling speed of an aero plane is determined by wing loading. Classification of UAVs based on working loading is presented in the table below:

Category	Wing loading kg/m^3	Example
Low	< 50	Seeker
Medium	50-100	X-45
High	>100	Global Hawk

Figure 3 Classification by Wing Loading

2.3.5 Classification based on platforms

There are three types of UAVs based on platforms: Fixed wing, Rotary wing and Hybrid UAVs.

2.3.5.1   Fixed wing

Fixed wing UAVs are similar to aircrafts in design with wings attached to the fuselage. These UAVs need launching and landing pads. These types of structures have high speed with greater endurance and range. Fixed wing drones cannot stay in one place with vertical lift rotors but instead they glide along a defined path (use energy to move forward) which makes this type of UAVs more efficient compared to rotary and hybrid ones.

Advantages

- They are able to cover long distances, map larger areas and loiter for long periods of observing their target.
- If these drones are gas powered, they can stay aloft for about 16 hours and the average flight time is only for two hours.
- They can fly at high altitudes fulfilling the surveillance and mapping purposes.
- They have the ability to carry more weight (high payload capacity)

Disadvantages

- They require large takeoff and landing zones for operation.
- These drones are expensive.
- They are unable to hover in one spot.
- Specific training is required to operate them (challenging to fly)
- These vehicles are less efficient for aerial mapping.

Examples of such UAVs are:

- CyberEye II
- Skywalker X8
- Predator A
- Global Hawk
- Harfang

Figure 4 Different Fixed Wing UAVs

2.3.5.2   *Rotary wing UAVs*

These are motor based structures in which motor is fixed on wings which provide thrust to give aircraft a lift. Tri-copters (with three rotors), quadcopters (with four rotors), hexa-copters (six rotors), are examples of rotary wing UAVs. These UAVs do not require any launching pad. Single rotors are similar in structure to helicopters. These drones have one big rotor at the center and small sized rotor on the tail for direction and stability. Tri-rotors are small in size and have longer flying times as compared to quad-copters and hexa-copters due to reduced number of motors.

Quadcopter uses four rotors with four propellers in which two motors rotate counterclockwise and the other two clockwise thus cancelling the torque from each motor (rotating in opposite direction). It is quite different from other vertical take-off and landing aircraft (VTOL) that the operator can use variable thrust between the four motors in order to control pitch, yaw and roll motion. Two

types of configuration are used in quadrotor: x-configuration and + configuration. x-configuration is more stable than + configuration which has more acrobatic construction. Two rotors on the opposite ends rotate in same direction while the other two rotate in opposite direction in + configuration. [2]

The quadcopter controlled motion is shown in figure below:
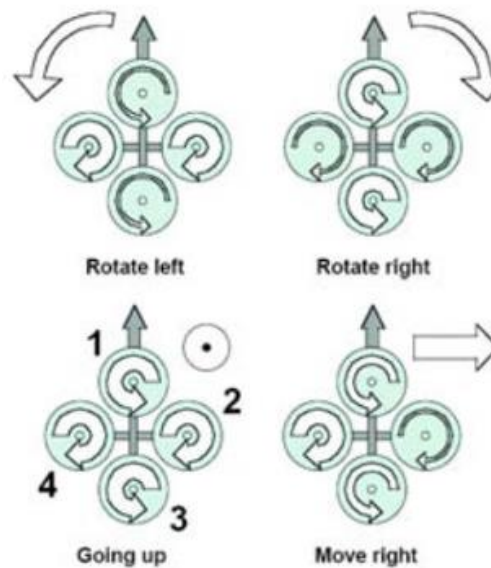
Figure 5 Quadcopter Controlled motion in different directions [2]

2.3.5.3   *Hybrid UAVS*

They are known as VTOL (vertical take-off and landing) i.e., they can also take off and land vertically. Motors are mounted on fixed wings providing a form of rotary motion. Rest of the structure is known as plane structure. It is a combination of fixed and rotary wing requiring both the features of fixed and rotary wing configuration. It does not require any sort of launching and landing pads.

Figure 6 Hybrid UAV (VTOL)

2.4 Structural Analysis Concepts

Finite element analysis is performed on the structure of UAV to check the reaction of substance with the real-world forces, physical effect. It provides a good information whether a substance will break, wear out, fail or work the way it was designed to be. Static structural analysis evaluates the displacements, stresses, strains, and forces induced in a structure or component by loads that do not create substantial inertia or damping effects.The analysis can validate structural rigidity and the maximum take-off weight the UAV can carry.

2.4.1 Structural components of fixed wing UAV

Following are the main structural components of fixed wing UAV:

2.4.1.1 Fuselage

Fuselage is the central body of the UAV. It provides structural connections for wings and tail assembly It can be truss type and skin stressed type. Truss type is made of beams, beams to resist loads. Members of truss are straight and connected at ends and load is applied at joints. Both compressive and tensile loads are applied on truss members. Skin stressed type includes monocoque structure semi monocoque structure. Load is taken up by the outer skin of the fuselage in monocoque structure. so, the strength of the skin must be high enough to resist the loads. Monocoque structure contains bulkheads, formers and skin. Concentrated loads are applied on bulkheads which are the heavy members of the fuselage. Formers are used in between bulkheads and skin to carry primary loads on fuselage.

Semi monocoque structure contains longerons and stringers. Extended members over the frame used to support the skin by taking the loads are longerons. Stringers are horizontal members used to attach skin with the fuselage. These are lighter in weight than longerons. Both longerons and stringers helps to control the fuselage bending by taking tensile and compressive loads. [3]

Monocoque and semi-monocoque structure configurations are shown in figure below:
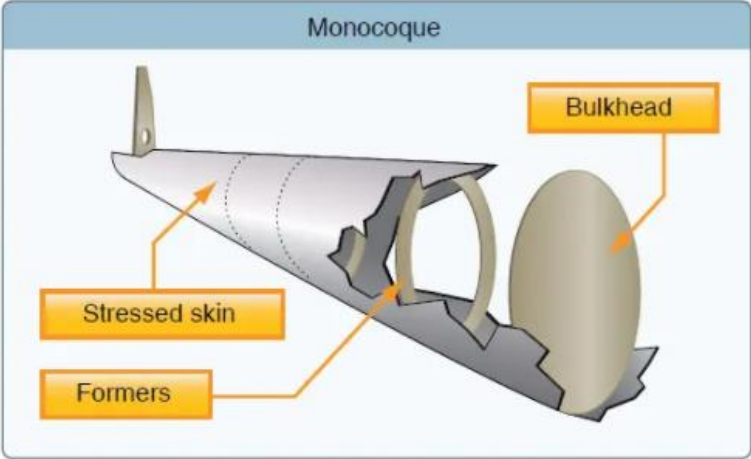
Figure 7 Monocoque Structure of Fuselage
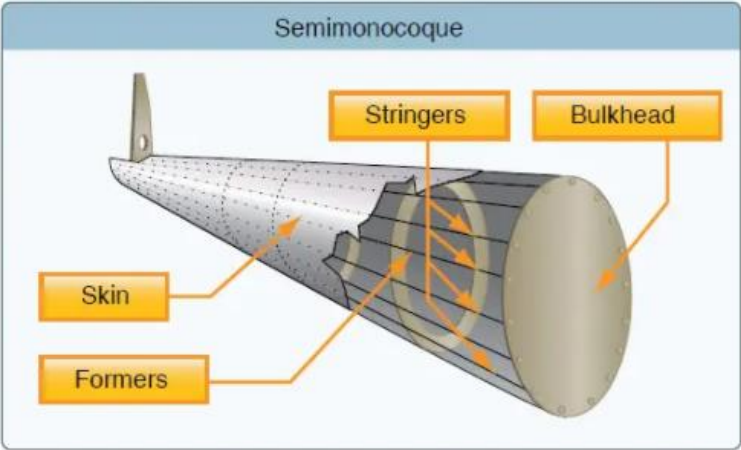
Figure 8 Semi Monocoque Structure

2.4.1.2   Wings

The major lifting surfaces of a UAV in flight are the wings, which are airfoils mounted to each side of the fuselage. High, mid, and low wings are attached to the upper, mid, and lower ends of the fuselage, respectively. External braces assist in spreading the load across the fuselage for added support. Semi-cantilever structures are what they're called. Spars, ribs, and stringers are the main structural components of wings. These are reinforced by trusses, I-beams, tubing, and other devices, including the wing skin. A wing's shape and thickness are determined by its ribs. Fuel tanks are an important part of the wing's design.

Ailerons and flaps are two types of control surfaces located on the front and back of the aircraft. Ailerons are aerodynamic forces that extend outward from the midpoint of each wing to the tip, moving in the opposite direction to allow the UAV to roll. The flaps on each wing extend outward from the fuselage to about midway. During cruising flight, the flaps are flush with the wing surface when fully extended. When the flaps are extended, they all travel downward at the same time, increasing the wing's lifting force during takeoffs and landings. [4]

In-detail structure of wing is shown in figure below:
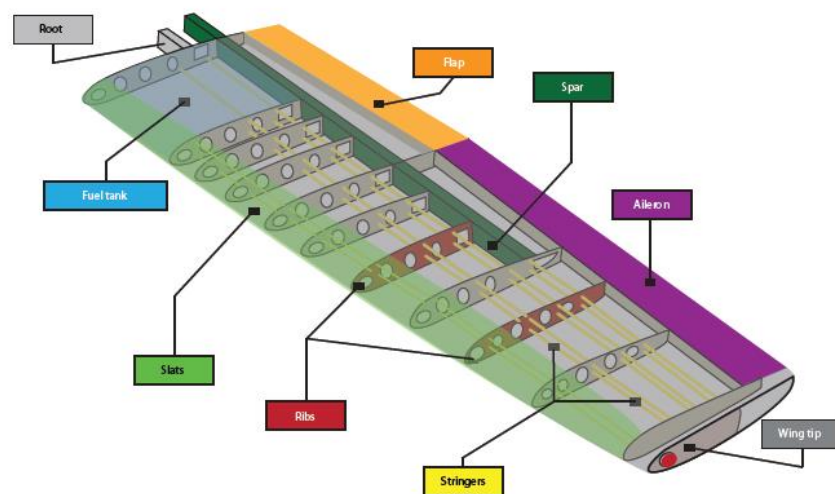
Figure 9 Structure of Wing [5]

2.4.1.3   Empennage

The empennage, which covers the entire tail group, is made up of the vertical stabiliser, horizontal stabiliser, rudder, elevator, and one or more trim tabs. The back of the vertical stabiliser is connected to the rudder. During flight, it is used to move the UAV's nose left and right. The elevator, which is connected to the back of the horizontal stabiliser, is used to raise and lower the UAV's nose during flight. Trim tabs are little moveable parts of the trailing edge of the control surface. These movable control tabs are moved by a human operator in the control room to reduce control pressures throughout the flight. Ailerons, rudders, and elevators all have trim tabs that can be fitted. [4] The configuration of complete empennage of UAV is shown in figure below:
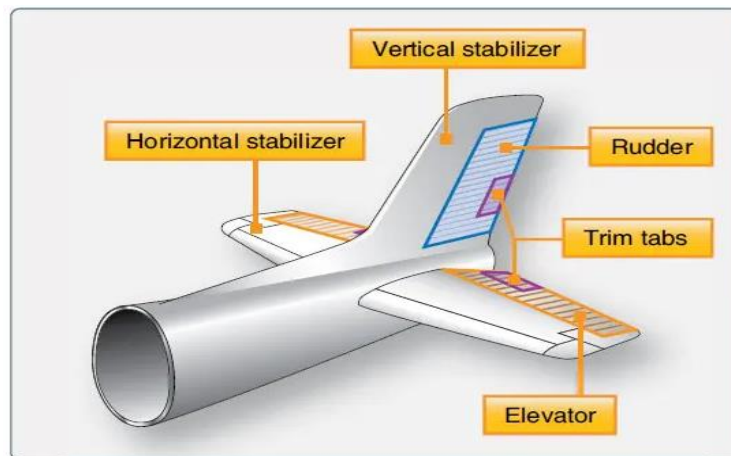
Figure 10 Empennage Structure Components [6]

The second empennage design does not necessitate the use of an elevator. Instead, a single-piece horizontal stabiliser pivots from the central hinge. The stabilator is a sort of design that is controlled by a control wheel, similar to how elevators are controlled. The stabilator pivots when the human operator pushes back on the control wheel, causing the trailing edge to go up. The nose of the UAV moves up as a result of this. Stabilizers have an anti-servo tab across their trailing edge instead of a trim tab. The anti-servo tabs travel in the same direction as the stabilator's trailing edge, reducing the stabilator's sensitivity. The anti-servo tabs also serve as a trim tab, allowing control pressures to be relieved and the stabilator to remain in the proper position. [4]

2.4.2 Loads applied on fixed wing UAV structure

Ground loads, such as taxing and landing loads, towing and lifting loads, are placed on the UAV structure during movement on the ground, whereas airloads, such as manoeuvres and gusts, are imposed on the structure during flight. These loads are further separated into surface forces, which include aerodynamic and hydrostatic pressure, and body forces, which act over the structure's volume and are caused by gravitational and inertial influences. Pressure distribution over the surfaces of skin causes air loads during flight, maneuver, or gust conditions. These effects cause direct loads, bending, shear, and torsion in all parts of the structure, in addition to localised normal pressure loads imparted to the skin. The structure is lifted by the wings, while the tailplane is used for directional control. Ailerons, elevators, and rudder aid in navigating and maintaining the stability of the UAV. [7]

2.4.3 Linear static analysis

This analysis is performed when linear elastic material (following a linear stress-strain curve behavior) is used. Loads are applied slowly. There is no extra vibration. In this analysis, force-displacement relationship remains linear and material behavior remains in elastic region. This analysis is generally valid for small deflections and rotations.

2.4.4 Non-linear static analysis

This analysis is performed for non-linear material. A material encountered high bending. In this analysis, force-displacement relationship is non-linear and material yields (plastic deformation). It is performed for moving parts, non-metallic materials such as composites or rubber, impact loads.

2.4.5 Dynamic Analysis

This examination is carried out in the event of an impact, such as when an aircraft is landing. The inertial and vibration impacts introduced into the system may be seen. Modal analysis aids in the discovery of the system's inherent frequencies without the need of any external force. Mode shape corresponding to each natural frequency can be obtained using modal analysis. Harmonic analysis is used in conjunction with modal analysis to analyze the system's harmonic response by determining the maximum deformation (amplitude) of the structure and checking for resonance criteria by comparing the highest applied excitation frequency to the structure's natural frequency. Dynamic loads are applied in a time or frequency-dependent manner. The amplitudes of the load

change dramatically over time. In comparison to static analysis, it is a more complex and realistic analysis.

2.4.6 Bending load on wing

It is a bending load case in which one end of the wing is fixed and load for bending is applied to the bottom of the wing. The pressure load, obtained from CFD analysis results in the form of pressure contours, is applied on wing structure. The pressure load induces bending in the wing. This will result in deformation of wing from its free end and stress concentrations start appearing from the fixed end towards the free end.

2.4.7 Torsional load on wing

In this case, the wing is again fixed from its root. An upward pressure load is applied on the top of the wing in the front half and the bottom of the wing in the back half is subjected to a a downward pressure load. This will induce twisting in the wing.

2.4.8 Meshing

Computational meshing of structure is done to find the required deflections and generated stresses in the structure against the loads applied. Different types of meshes can be used with 2D (quadrilateral/triangular/rectangular etc.) or 3D elements (tetrahedron, hexahedron, pyramid etc.) depending upon the dimensionality of finite element model made on analysis software. Mesh refinement can be carried out in regions where accurate results are the requirement. Transition elements (triangular elements) are used where material properties change, thickness in the structure changes, concentrated loads are applied etc. Brick elements are also used in some analysis of wings. volumetric mesh for some 3D wing structure is carried by first meshing the airfoil plane area then extrudes it along the span known as volumetric meshing with hexagonal mesh elements). In some analysis, it is found out that ribs, spars and skin are modelled with different elements. 1D beam element, 2D shell element, and 3D tetra elements can also be used to model wing structure.

2.4.9 Materials

Generally, material used in finite element modelling is isotropic (A material whose properties remain same in all directions). For ductile material properties like Yield stress, Young's Modulus,

Poisson's ratio, material density is defined in simulation setup as they directly influence the material behavior when external loads are applied to it.

2.4.9.1 Aluminum

Aluminum alloys are used to manufacture wings of UAVs. Properties like high strength to weight ratio, resilient, ductile at low temperatures, corrosion resistant, non-toxic, light weight make aluminum the best material to be used in wing structures. Aluminum alloys including 6061-t8 are generally used for wing structures with tensile yield strength of 276 MPa and an ultimate tensile strength of 310 MPa. For front, rear spars and bottom skin in wings, Aluminum 2024 can be used as it has better resistance towards fatigue with good machinability. For top skin, the best aluminum alloy is Alum.7050 having high strength durability within its life span. Its maintenance is quite easy as it is a stable alloy. Aluminum 7075-T651 can be chosen for brackets region as it has high strength to weight ratio and high stress concentrations. Rivets use aluminum material for its high strength to weight and have dim dimples. Materials used in different parts of wing structure are represented in the table below:

2.4.9.2 Steel

Bolts for brackets are generally made of AISI-8740 steel as they have high strength and toughness along with hardened ability. However, they are low in corrosion, but this can be prevented all with protection using alloyed steels.

2.4.9.3 Titanium

Titanium alloys have excellent specific characteristics, a good fatigue strength/tensile strength ratio with a definite fatigue limit, and some retain significant strength at temperatures as high as 400–500 degrees Celsius. Although characteristics are substantially damaged by exposure to temperature and stress in a salt environment, there is generally good corrosion and corrosion fatigue resistance. Generally, ribs and spars of wing structure are fabricated using titanium alloys. Titanium alloys have a relatively high density, which means that if the alloy is used extensively, weight penalties will be imposed, as well as high manufacturing costs, which are around seven times those of aluminum and steel.

2.4.9.4   *Composite materials*

Composite materials, mainly CFRP (carbon fiber reinforced polymer with epoxy as matrix) are used in fuselage structures of UAV. Carbon fibers with epoxy resin (matrix) with density of 1.60 g/cc, Young's Modulus 70.0 GPa and Poisson's ratio of 0.3 give good structural analysis results for fuselage. Composite materials are made up of strong fibres like glass or carbon that are wrapped in a plastic or epoxy resin matrix that protects them mechanically and chemically. The fibres might be continuous or discontinuous, but their strength is significantly greater than that of the bulk materials. Carbon fibres, for example, have a tensile strength of around 2400 N/mm^2 and a modulus of elasticity of about 400 000 N/mm^2.

Fiberglass is another option. The direction of the fibres determines the features of an anisotropic sheet of fiber-reinforced material. Two or more sheets are sandwiched together to form a lay-up in structural form, with the fibre directions matching those of the heavy loads.

The ply stacking sequence for composite materials is determined by first determining the principal load direction acting at a given location. The fibre orientation may then be altered to its direction, allowing for efficient load transfer. The optimal ply configuration for an aircraft composite wing is [0/90/45/-45/90/0].

Following is the table showing the material used in composite UAV wing with different ply orientation:

Part	Material	Ply Orientation
Upper Skin	Plastic Film	-
Lower Skin	Plastic Film	-
Front Spar	Woven Carbon Epoxy	$[90_2/0_2/45_2/-45_2]_s$
Joiner	Woven S-Glass Epoxy	$[90_2/0_2/45_2/-45_2]_s$
Rear Spar	Aluminum 6061 T6	-
LE (curved)	Woven Carbon Epoxy	$[90_2/0_2/45_2/-45_2]_s$
LE (flat)	Balsa	-
Ribs	Woven Carbon Epoxy	$[90/0/45/-45]_s$

Figure 11 Composite materials with Ply Orientation [1]

2.4.9.5   *Balsa wood*

Balsa wood can also be used in wing structures. Its softness and flexibility makes it perfect for model building of aircrafts or UAVs.

2.4.10   Boundary Conditions for HALE UAV

For early study of HALE UAVs, non-linear Prandtl Lifting line theory (NLLT) is often recommended. Following NLLT, we may apply Spanwise lift distribution along one-half wing span. In addition to lift force, the wing structure is subjected to gravity and any other focused loads. The structure's weight is determined automatically using the material density entered into Ansys Mechanical pre-processing. The ribs at the wing root are subjected to a fixed support boundary condition, which prevents translation and rotation in all directions. The wing tip, on the other hand, is unrestricted in all degrees of freedom.

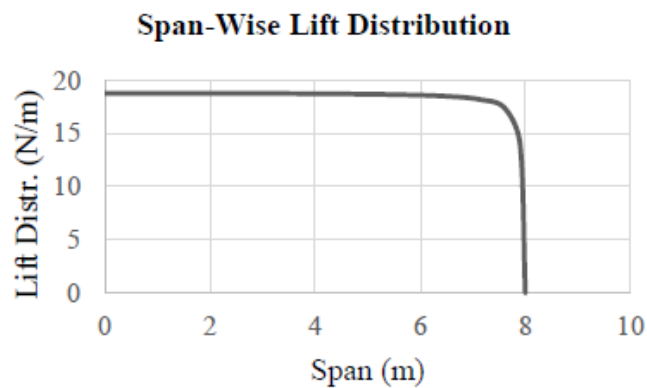Span wise Lift distribution for HALE UAV is shown in figure below:

Figure 12 Span-wise lift distribution for HALE UAV [1]

2.4.11   Stresses

Finite element analysis gives us good overview of how stresses generate in the structure. These stresses. Von misses stresses give the regions of stress concentrations while principal stresses show the direction of stresses generated. The Von Mises stress is a metric for determining whether a material may yield or fracture. It's most frequently utilized on ductile materials like as metals (Aluminum). According to the von Mises yield criteria, a material will yield if its von Mises stress under load is equal to or greater than its yield limit under simple tension.

2.4.12   Failure Criteria

Failure criteria is used to guarantee that a UAV structure can withstand the loads it is subjected to, regardless of whether it fails. Based on the material property, there are many distinct types of failure criterion. The Tsai-Wu failure criteria are used for parts made of composite materials, while the Von-Mises failure criteria are used for isotropic or homogeneous materials. The Tsai-Wu failure criteria is more sophisticated and broader since it distinguishes between compressive and tensile strength of a lamina. The Tsai-Wu failure criteria are based on Beltrami's strain energy failure concept. [1]

2.4.13   Safety Factor

The safety factor is defined as the difference between Von-Mises stress (VM) and the material's allowed stress (yield stress/Y) (SF).

$$\text{SF} = \frac{\sigma_Y}{\sigma_{VM}}$$

If the safety factor is larger than one, the structure is safe. Otherwise, a safety factor of less than one indicates that the structure has undergone unfavourable plastic deformation. [1, Research paper]

2.5   Fluid and Aerodynamic Concepts

2.5.1 Lift

Lift is achieved by creating a differential pressure distribution on the object's 'top' and 'bottom' surfaces. It acts normal to the free-stream velocity of fluid. The shape of an item has the greatest impact on its lift, including orientation of this shape with respect to the freestream flow direction. Secondary influences include Reynolds number, Mach number, and the surface roughness.
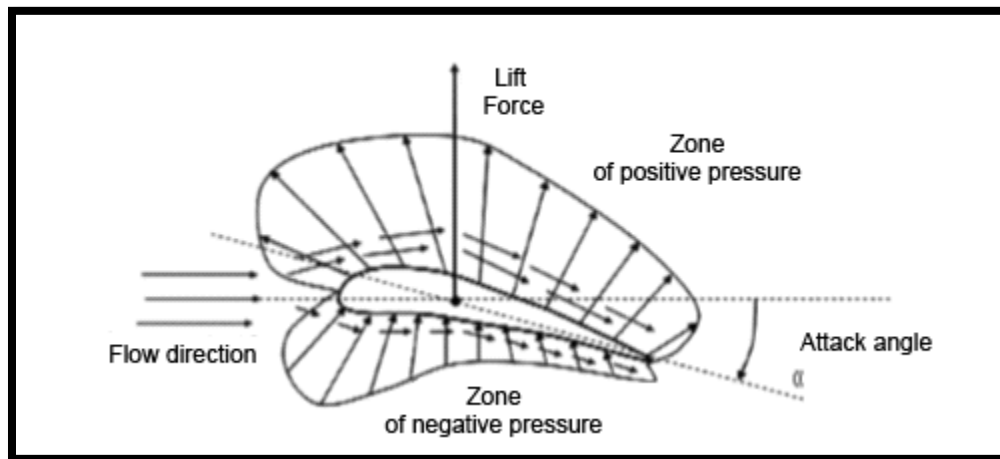
Figure 13 Principle of Lift generation.

2.5.2 Drag

Drag is the resisting force created when a body moves through a fluid. It works in the same direction as free-flow fluid motion. The shape of the object, Reynolds number, and other characteristics like surface roughness all impact drag. In actual viscous flows, it is always non-zero and is made up of two parts:

- Friction or viscous drag is caused by tangential shear strains acting on the object. Flows past streamline bodies like airfoils or wings have this drag as a dominant component.

- The normal stress applied by the pressure forces causes pressure drag, which becomes dominant in flows past bluff bodies. Because of its great dependence on the shape of the body, it is commonly referred to as form drag

Figure 14 Aerodynamic Forces on an airfoil.

2.5.3 Angle of Attack and Stall

"Angle of attack (AOA) is defined as the angle between the direction of upstream flow and the reference line of the body (usually cord of an airfoil)."

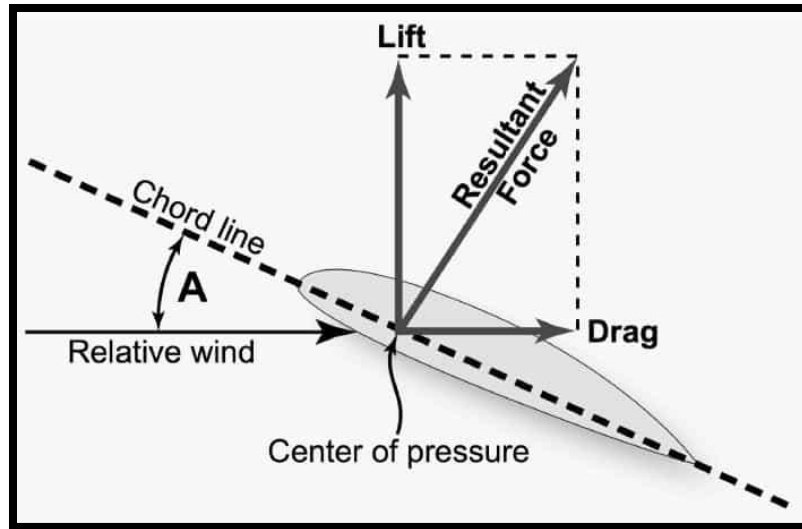A symmetric airfoil cannot produce lift at AOA = 0 deg because pressure forces on both sides will be equal. Therefore, a symmetric airfoil must be at positive AOA to generate lift. On the other hand, a non-symmetric airfoil can generate lift even at AOA = 0 deg. The asymmetry or camber between the two surfaces of the airfoil leads to unequal pressure distribution, resulting in non-zero lift force. A wing is complexly designed to optimize lift and minimize drag, and different sections can have different airfoil profiles.

For airfoils, lift is proportional to the AOA for small angles within ~10 degrees. As the AOA reaches a critical value, there is a sudden drop in lift, called wing stall. Stall is caused by the flow separation which changes the flow dynamics on the suction side of the wing. Moreover, it increases the drag due to sudden generation of a large wake on the rear side of the wing.
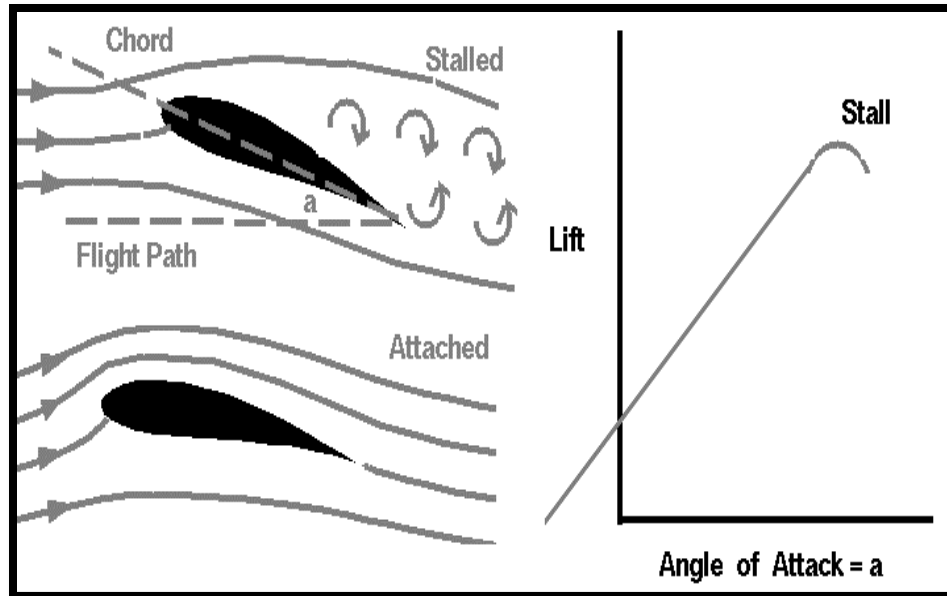
Figure 15 Angle of Attack and Stall of an airfoil.

2.5.4 Airfoil Selection:

2.5.4.1   Selection Criteria:

The airfoil selected depends upon the selection criteria that is employed. The selection criteria are a collection of design requirements. Following are some of the selection criteria employed:

1. Airfoil selection on the basis of highest maximum lift coefficient (Cl max).
2. Selecting an airfoil based on the lift coefficient that is closest to a certain determined design lift coefficient (Cl d or Cl i) at different angle of attacks.
3. Selecting an airfoil with the minimum drag coefficient (Cd min).
4. Selecting an airfoil with the highest lift-to-drag ratio ((Cl /Cd) max)
5. Selecting an airfoil based on the highest lift curve gradient (Cl gradient).
6. Selecting airfoils with low pitching moment coefficient (Cm).
7. Selecting an airfoil in which the stall quality varies gently rather than sharply in the stall region.
8. Selecting an airfoil that is structurally sound and capable of handling the highest pressure it is likely to experience during its operation.

9. Selecting an airfoil keeping in mind the ease in manufacturing. Airfoils can be extremely precise and may require a lot of time, money and a specialized manufacturer to manufacture properly.
10. Cost based selection.

A unique airfoil which provides optimum values for all of the above given criteria does not exist and a compromise needs to be reached on which design criteria is most important. An airfoil may have the highest maximum lift coefficient Cl max, but not the highest value of maximum lift to maximum drag ratio. A compromise must be made through a weighting process, in which certain design criteria are given a greater importance compared to others

2.5.4.2 NACA airfoils:

The analysis of the flow around an airfoil necessitates the exploration of numerous hypotheses while designing an air foil from the ground up. However, because it takes a lot of time and work, we decided to employ airfoil design equations produced by the National Advisory Committee for Aeronautics (NACA) to create our airfoils.

One of the most dependable and extensively used airfoils is one created utilizing NACA derived equations. NACA was founded in 1915 before being disbanded in 1958 in favor of the creation of NASA, the National Aeronautics and Space Administration. The following airfoils are widely used;

- Four-digit NACA airfoils
- Five-digit NACA airfoils
- 6-series NACA airfoil

Four-digit airfoils are represented using four digits (e.g. 1075) while five-digit airfoils are represented by five digits (e.g,17869), while the 6-series airfoils are represented such that their name begins with the number six.

As in our project we'll be using the four-digit airfoil. Hence, in the literature review we'll be discussing in detail just the four-digit airfoil.

2.5.4.2.1 Four-digit NACA airfoils:

In a four-digit NACA airfoil, each digit represents a unique parameter or feature of the airfoil:

1. 1. The maximum camber of the airfoil is expressed as a percentage of the chord length of the airfoil.
2. 2. The second value indicates the percentage distance along the chord where the airfoil's greatest camber occurs.
3. 3. The last two figures represent the airfoil's maximum thickness as a percentage of the chord length.

For example, a NACA 4415 airfoil section (see image below) has a maximum thickness to chord ratio (max t/c) of 15% (last 2 digits), a maximum camber of 4% of the chord length, and a maximum camber of 40% along the chord length.
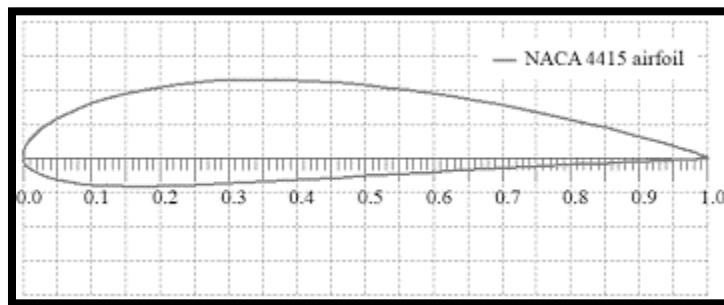
Figure 16 NACA airfoil selection

2.5.5 Turbulence Models

A number of different turbulent models are available in Ansys like k-epsilon, k-omega, Realizable k-epsilon, SA, SST-k ω etc. Two of these are more suitable for our analysis of UAV which is essentially an external aerodynamics problem:

2.5.5.1   Spalart – Allmaras (SA) Model

This turbulence model involves one transport equation for kinematic eddy viscosity parameter and specifying the length scale by means of an algebraic formula. SA model requires no wall functions and shows good performance in boundary layers with adverse pressure gradients. Because of its applicability for airfoil applications, the SA model is gaining popularity in the

turbomachinery field. However, it does not perform well for some general industrial flows like free shear flows, particularly plane and round jet flows.

2.5.5.2   Menter SST k-ω model

The k– model's findings are less susceptible to the beginning circumstances, but its near-wall performance for boundary layers with unfavourable pressure gradients is inadequate. As a result, a hybrid model may be utilised, with the k– model in the near-wall zone and the standard k– model in the totally turbulent region distant from the wall. SST k-omega turbulence model is preferred for our analysis because:

- For exterior aerodynamics, the SST k-model is the most accurate 2-equation RANS turbulence model in Fluent.
- It performs better for wall-bounded boundary layer, free shear, and low Reynolds number flows when compared to models from the k-family.
- It is great for intricate boundary layer flows with adverse pressure gradients and separation when compared to standard k-family models.
- Predicts flow separation more accurately than other RANS models with two equations.

2.5.6 Dimensionless Parameters

2.5.6.1   Reynold's Number

Reynold's number (Re) is a dimensionless parameter which is used for the characterization of fluid flow i.e., whether the flow is laminar or turbulent. It is defined as the ratio of inertial forces to viscous forces and is given by the formula:

$$Re = \frac{\rho u L}{\mu}$$

Where ρ is fluid density, L is characteristic length, u is fluid velocity and μ is the viscosity of fluid. The flow is laminar for low Reynold's numbers and becomes turbulent at relatively large Re. For example, consider the case of flow inside a circular pipe. If Re<2300, the flow is laminar, for 2300<Re<4000 it's transitional and it becomes turbulent for Re>4000.

2.5.6.2   Courant Number

While numerically solving certain partial differential equations, the Courant–Friedrichs–Lewy or CFL condition is required for convergence (like hyperbolic PDEs). The Courant number is a dimensionless quantity that reflects the amount of time a particle spends in a single mesh cell.

It must be less than one and is normally kept at less than 0.7. When the Courant number exceeds 1, the time step is too big, and the solver may 'skip' certain cells.

2.5.6.3   *Lift and Drag Coefficients (C_L and C_D)*

Drag coefficients, C_D for most external flows depend primarily on the Reynolds Number. The drag coefficients for some common shapes can be found in tables. For more complex geometries, drag forces can be obtained using experiments or computational fluid dynamics simulations.

The lift coefficient, C_L is a dimensionless coefficient that relates the lift generated by a lifting body to the fluid density around the body, the fluid velocity and an associated reference area. Mathematically, it is given by:

$$C_L = \frac{F_L}{1/2 \, \rho V^2 A}$$

The lift-to-drag ratio is the lift created by an object divided by its drag. This is an indication of the aerodynamic efficiency of an airplane. One of major objectives of aircraft design is higher lift-to-drag ratios. High-performance wings generate lift which is on the order of two orders of magnitude higher than their drag.
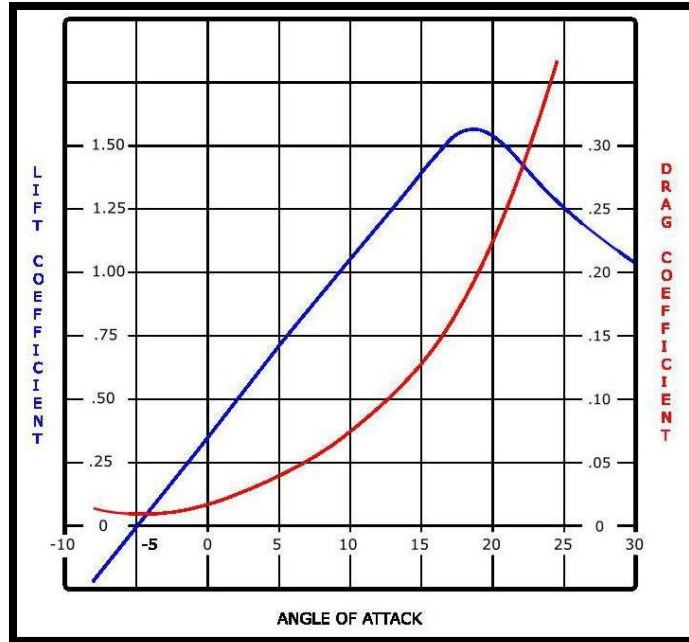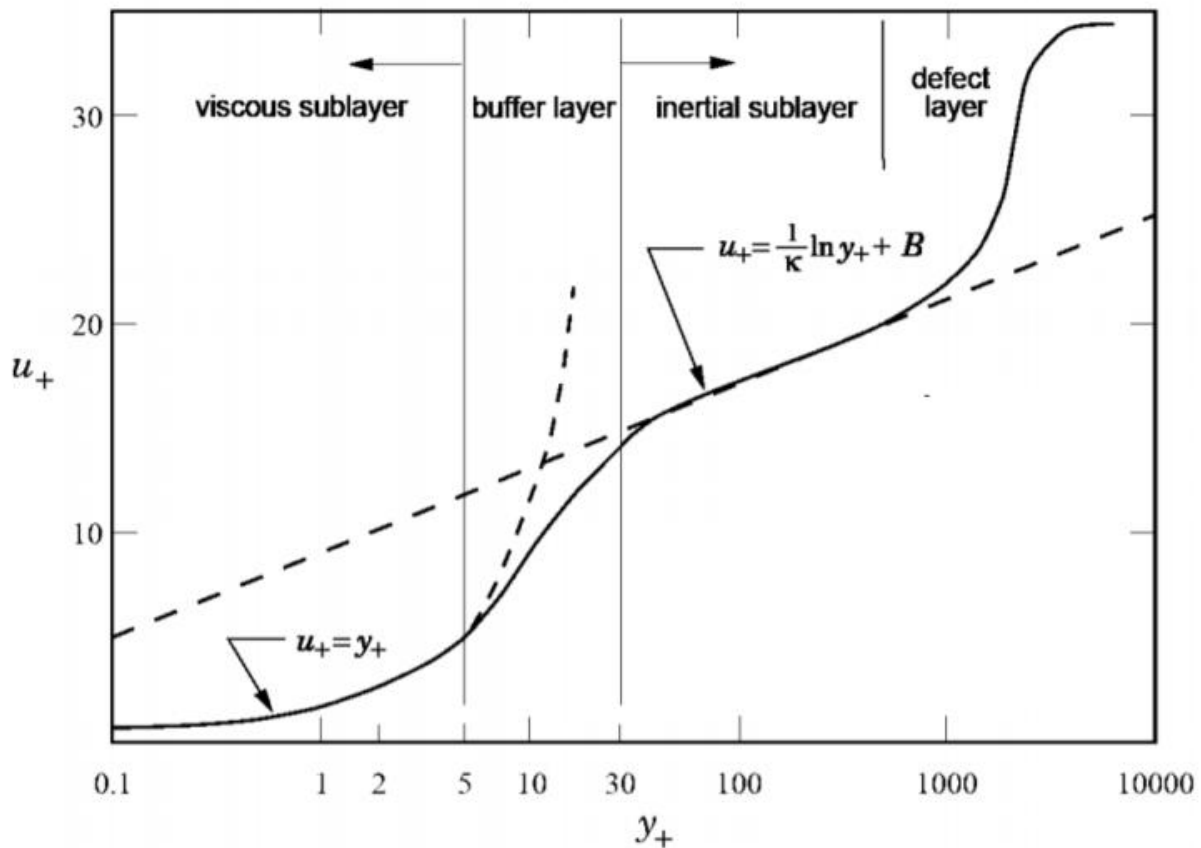
Figure 17 Lift-to-drag ratio vs angle of attack.

2.5.6.4 *Wall modelling and y^+*

We use wall modelling for a realistic simulation of the boundary layer, especially in case of external aerodynamics. The 'Law of Wall' is a specific way of describing velocity close to the wall and is given by:

$$\mathbf{u}^+ = f(\mathbf{y}^+)$$

where u+ is a dimensionless velocity and y^+ being a dimensionless wall distance.

Figure 18 Near wall region and Law of wall.

y^+ is a dimensionless number and describes which particular region of the boundary layer is solved. It depends upon the fluid viscosity as well as the velocity and first-cell distance close to the wall:

$$y^+ = \frac{y\, u_T}{\nu}$$

Where u_τ is the so-called friction velocity, y is the absolute distance from the wall and ν is the kinematic viscosity.

Actually, RANS assume a fully turbulent flow and thus, performs poorly near the wall. In order to deal with the near wall region, the turbulence models are modified to enable the viscosity-affected region, which includes the viscous sublayer, to be resolved with a fine mesh near to the wall. When solving the near-wall area, the first cell center must be located in the viscous sublayer (preferably $y^+ = 1$)

3 CHAPTER 3: METHODOLOGY

The general approach we adopted towards our project is can be shown as:
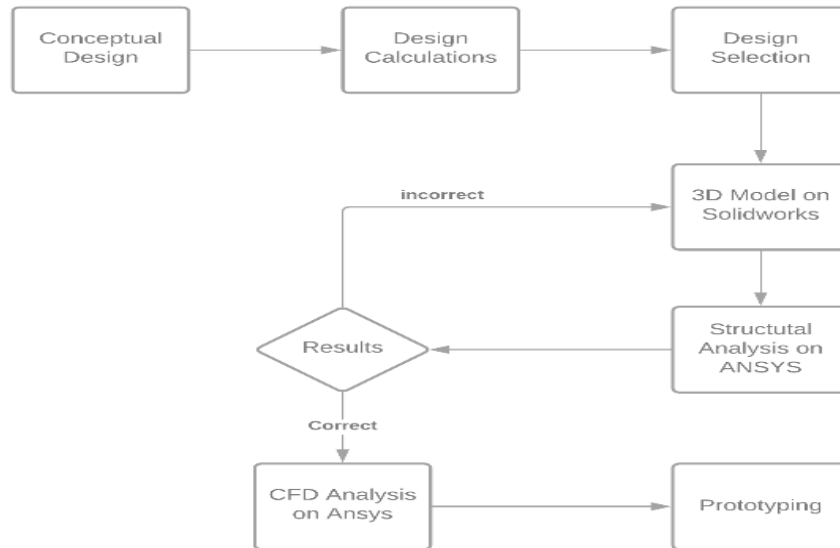
Figure 19 General Approach

3.1 Conceptual Design

First, we made conceptual design according to our design specifications that were provided to us. The conceptual designs are hand-drawn and they are inspired from different UAVs that are already present. The design specifications are as below:

Length	4m
Width	0.5m
Wingspan	3.5m
Tail Configuration	X-tail
Weight (Dry mass)	300 kg
Altitude	8000-10000m
Range	150 km
Power source	Battery operated

Table 3 Design Specifications

Keeping in view, we will make three conceptual designs and then we will select design and then use it for analysis and prototyping. Three designs we have created are as follows:
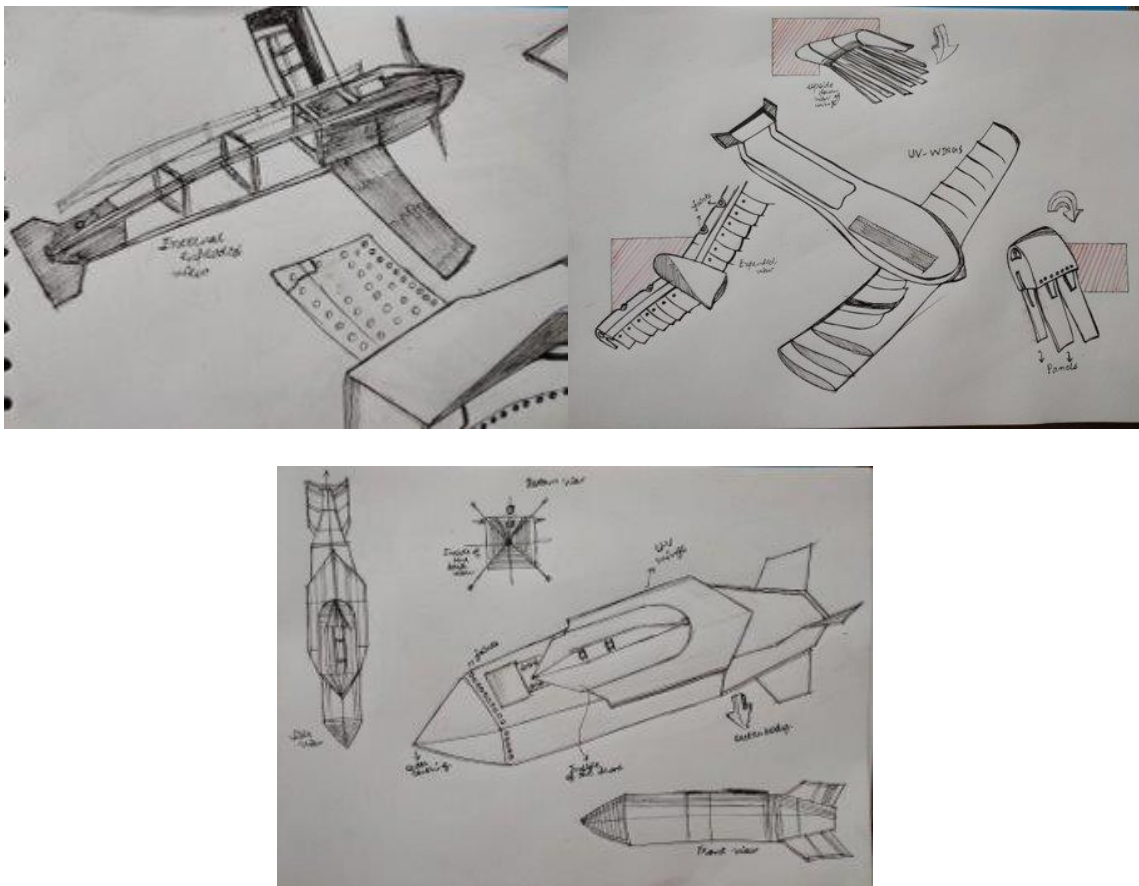

Figure 20 Conceptual models

3.2 Wing Loading Design Calculations

The overall mass of an aircraft (UAV) divided by the area of its wing is referred to as wing loading. Wing loading can also be used to calculate an aircraft's stalling speed. Because larger wings move

more air, a UAV with a large wing area compared to its mass will stall slower. As a result, planes will be able to take off and land at a lower speed or take off with a heavier load. It will be able to turn at a faster rate as well. Gust response (how sensitive a UAV is to changes in air density and turbulence) is also influenced by wing loading. A wing with a limited area and low wing loading will be subjected to a rough and strenuous ride during flight. Wing load calculations are shown as below:

Wingspan= b = 3.5 m

Root Chord length Cr= 0.7 m

Tip chord length Ct = 0.7 m

Considering taper ratio to be 1.

Taper ratio = λ = Ct/Cr = 1

Wing area = S = b*C

Where C is average chord.

$$C = (\frac{2 * Cr}{3})(\frac{1 + \lambda + \lambda^2}{1 + \lambda})$$

Since λ = 1, the above equation reduces to C = Cr

Hence wing area will be S = b*Cr = 3.5*0.7 = 2.45 m2

Body mass of UAV in kg = W = 300 kg

Hence, Wing loading is = mass of UAV/wingspan area = 300/2.45 = 122.45 kg/m2

In weight terms it is 1201.22 N/m2.

We can see that wing with larger wing area relative to its mass will have low wing loading as compared to one with high wing loading. UAV with higher wing loading will fly faster. Increased wing loading also increases takeoff and landing distance. Maneuverability also decreases with high wing loading.

3.3 Design selection

There are some design considerations that are to be kept in mind while selecting our design staying in the specifications that were provided to us. These specifications include wing configuration, straight wing, tail configuration

3.3.1 Basic airframe configuration

There are three fundamental airframe configurations that are taken into account. There are four factors to consider: manufacturing process ease, stability, hand launch ease, and mass. The comparison of the three basic airframe configurations is shown in the table, with configuration five being the best and configuration one being the worst. The horizontal tail is located at the back of the fuselage in the traditional form. Both the horizontal and vertical tails can be connected.
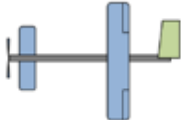
Design Parameters	Weight	Conventional	Canard	Flying Wing
Ease of manufacturing process	0,3	4	3	5
Stability	0,3	5	4	2
Ease of hand launch	0,2	5	5	4
Mass	0,2	4	4	5
Total Σ (weight x value)	1	4,5	3,9	3,9

Figure 21 Comparison of basic airframe configuration.

3.3.2 Wing configuration

There will be three vertical wing locations against the fuselage to consider. The simplicity of manufacture, stability, hand launch ease, and ground clearance are all factors to consider. The three vertical locations of the wings in relation to the fuselage are shown in the table. The high wing design has been chosen for our research.
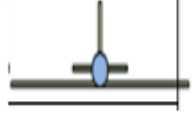
.

Design Parameters	Weight	High Wing	Mid Wing	Low Wing
Ease of manufacturing process	0,3	5	3	4
Stability	0,3	5	4	3
Ease of hand launch	0,2	5	4	3
Ground Clearance	0,2	5	4	3
Total Σ (weight x value)	1	5	3,7	3,3

Figure 22 Comparison of wing configuration

3.3.3 Planform

When viewed from above, a planform is the shape of a wing. The comparison of the three straight wing planforms is shown in Table 3. The rectangular wing is inferior to two other wing

planforms in terms of aerodynamics and structural. According to our needs, we'll employ prismatic mid-section for our research.

Design Parameters	Weight	Rectangular	Tapered	Prismatic Mid-Section
Ease of manufacturing process	0,6	5	3	4
Strength of structure	0,2	4	5	5
Aerodynamic performance	0,2	3	5	4
Total Σ (weight x value)	1	4,4	3,8	4,2

Figure 23 Comparison of straight wing.

3.3.4 Tail configurations

There are three different tail layouts to examine. X-tail, T-tail, and V-tail are the three tails. The simplicity of the manufacturing process, the weight structure, and the aerodynamic performance are all factors to consider. The comparison between the three tails is shown in the table. In our design, we'll employ X-tail arrangements. Because of its simple, lightweight, and strong structure, this configuration is straightforward to construct.

Design Parameters	Weight	X-tail	T-Tail	V-Tail
Ease of manufacturing process	0,4	5	4	4
Weight of structure	0,4	5	3	5
Aerodynamic performance	0,2	4	5	3
Total Σ (weight x value)	1	4,8	3,8	4,2

Figure 24 Comparison of tail configuration

3.4 3D model on Solid works

After selecting all the design parameters, we will create the 3d model on Solid works. The assembly we have created includes all the joints of individual parts. The model is designed so we can perform analysis on Ansys later on. The 3d model is shown as below:
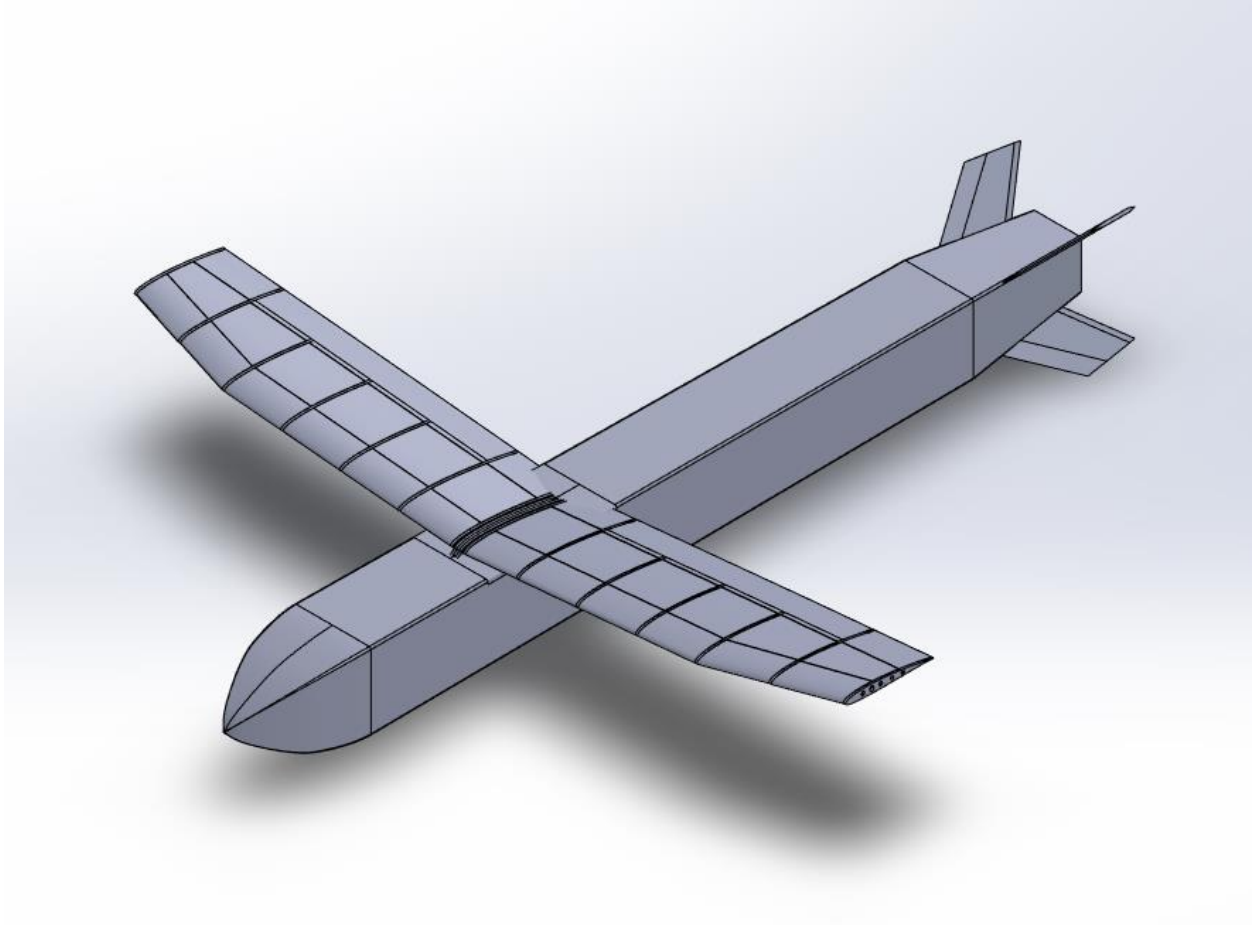
Figure 25 Isometric view of 3D model

This is the interior design of the model. The ribs and spars of models can be seen where we will place our batteries, motors, control system assembly and cameras. The reason we create this structure is to give stability to our model. This helps our design in structural analysis as stress concentration becomes low. The deformations also become less this way. The other views of our Solidworks model are shown as below:
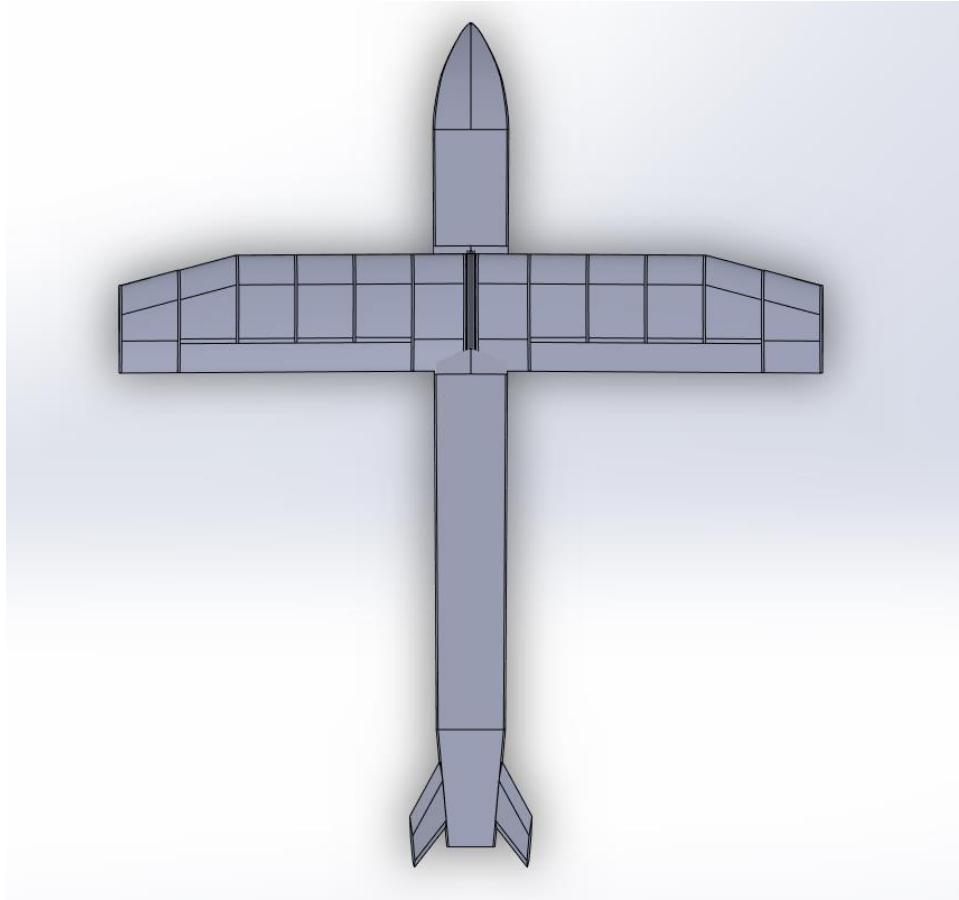
Figure 26 Top View

Figure 27 Front view

3.5   Aerodynamic Analysis

3.5.1 Fluid domain:

A fluid domain in CFD analysis is a virtual wind tunnel i.e. we simulate our model as if being tested inside a wind tunnel. As per the practices found in the literature, the upstream length is taken 7L (where L is characteristic length, being the length of uav in our case). Similarly, the vertical and transverse lengths are taken as 5L. However, the downstream length is taken as 15L since the body is expected to shed a wake of lower energy flow in this region.
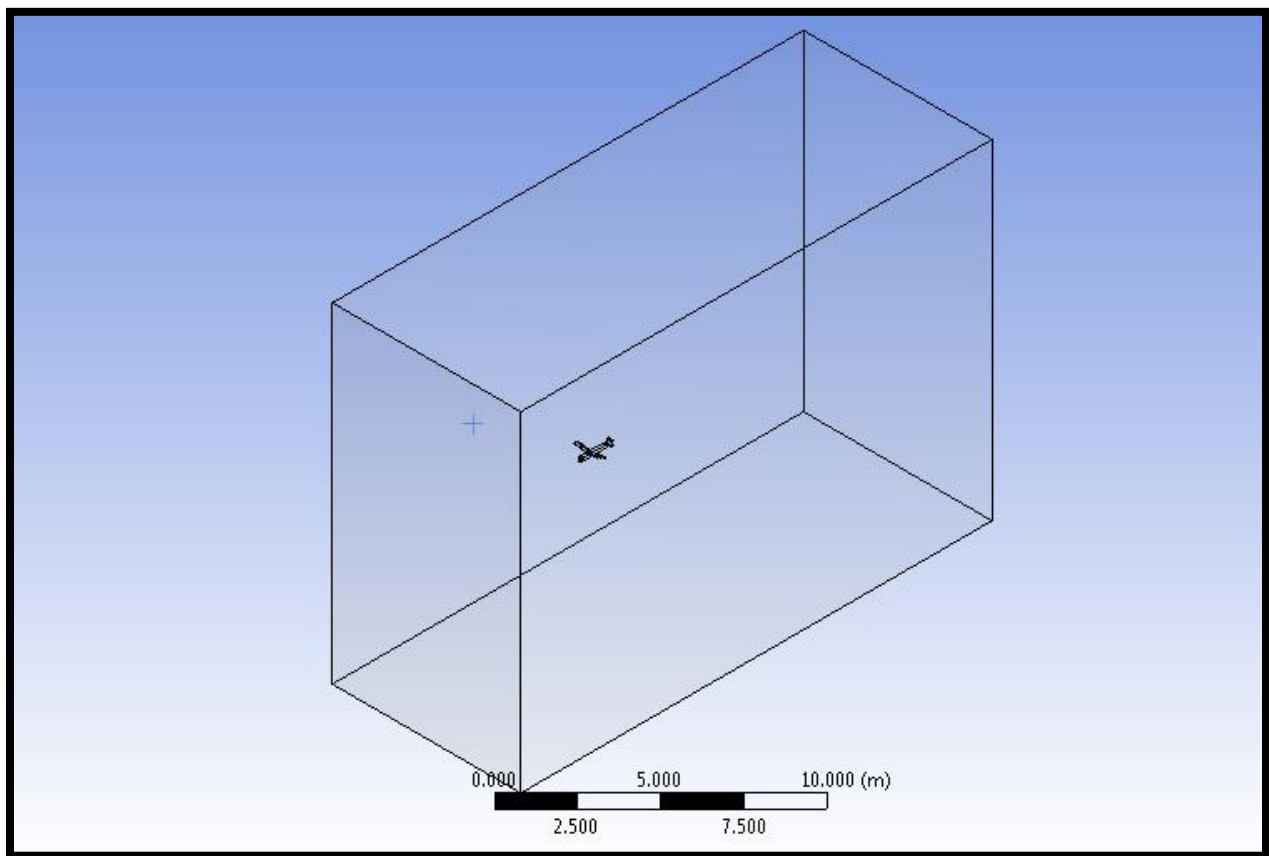
Figure 28 Fluid domain

3.5.2 Meshing:

An unstructured (tetrahedral) mesh of maximum element size 0.3m is used along with refinement around the uav body. Moreover, necessary refinement is done on the downstream region as well, to properly capture the wake regions and other important fluid phenomena. This resulted in around 1.5M elements with 38,000 nodes. The results are also obtained for 2M and 3M mesh elements to confirm the mesh independence (discussed later in the report).
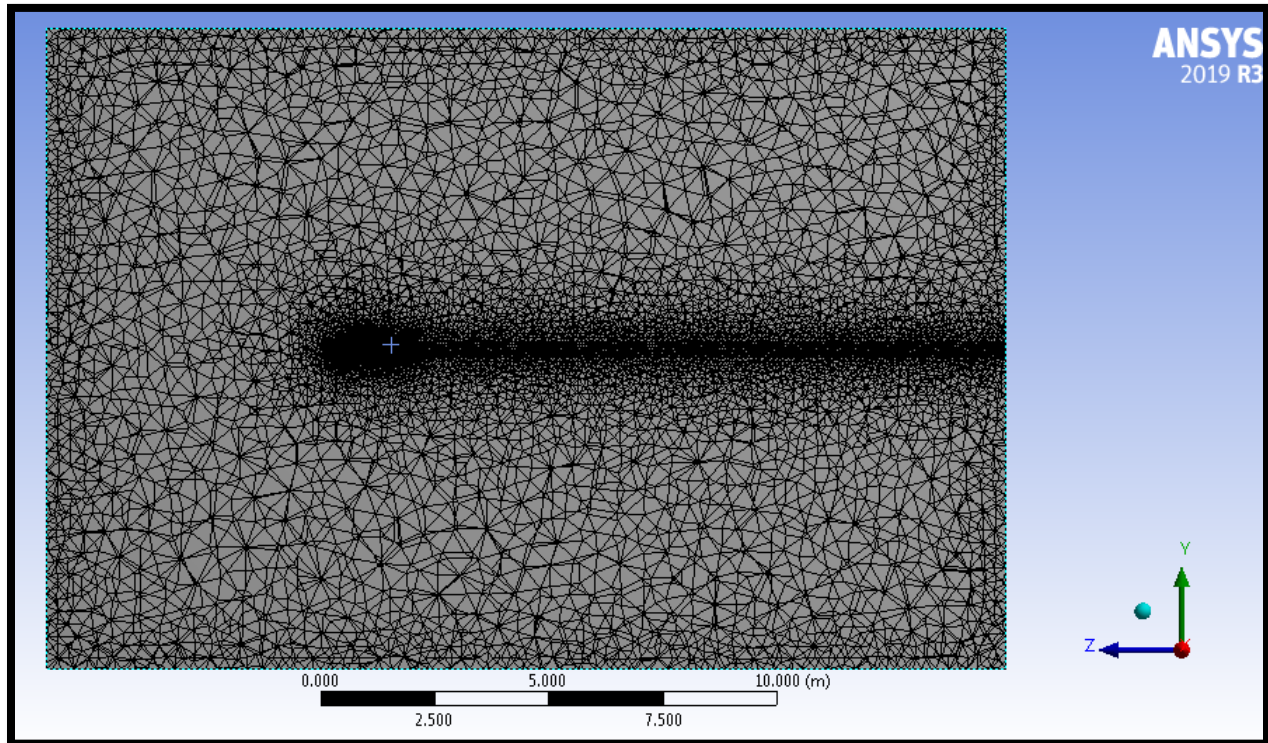
Figure 29 Meshing

3.5.3 Inflation layers:

Inflation or prism layers are used because inside the boundary layer, there is a steep change in velocity in the vertical direction while the profile is nearly same in the horizontal direction. Therefore, to properly resolve this gradient, the cells need to be smaller normal to the wall (uav in our case) than along the wall.

The two important parameters to choose were the first cell height, y_H and the growth ratio G. As per the desired y+ of 1, a first cell height is computed to be 2.38e-6 (htt). Whereas a growth ratio of 1.1 is chosen compared to the default value of 1.2 in order to improve the solution accuracy.

The idea is to contain the entire boundary layer within the inflation layers. This is done by choosing 12 layers as given by the formula:

$$y_T = y_H * \frac{1 - G^N}{1 - G}$$

Where y_T is the total cell height, y_H is the first cell height, G is growth ratio and N is the total number of layers.
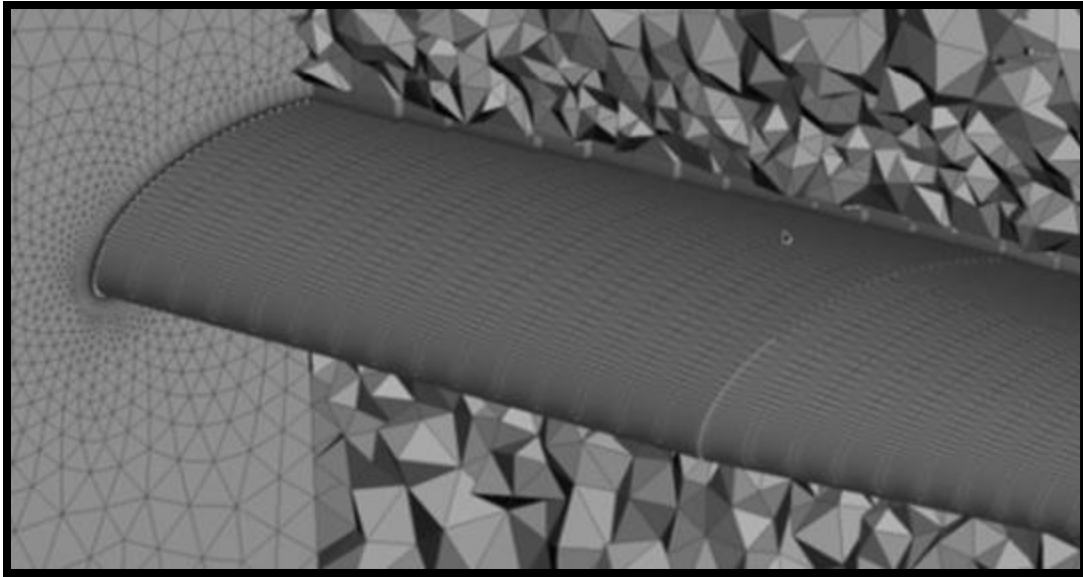
Figure 30 Wing-surface mesh with inflation layers

3.5.4 Atmospheric properties:

The UAV is simulated at two main scenarios of interest:

1. Sea-level conditions
2. Airborne at 6000m

The reference values can be found in a table in Appendix III.

Properties	Sea Level	6000m
Temperature (°C)	15	-23.96
Gravity (m/s²)	9.807	9.788

Static Pressure (Pa)	101,300	47,220
Air Density (kg/m$_3$)	1.225	0.665
Dynamic Viscosity (x10^{-5} Ns/m^2)	1.789	1.595
Reynolds Number	18.2 M	11.09 M

Table 4 Air properties

3.5.5 Problem setup and Boundary conditions:

Different parameters for problem setup in the Fluent along with the boundary conditions used are summarized in the table below:

Inlet	Velocity (190 ms^{-1})
Angle of attack	0-5 degrees
Outlet	Gauge pressure (0 Pa)
UAV body	Wall (no slip)
Domain boundaries	Wall
Model	Turbulence (kω-SST)
Solver type	Pressure based, steady
Scheme	Coupled

Table 5. Problem setup and Boundary conditions

3.6   Structural Analysis of UAV

Static structural analysis evaluates the displacements, stresses, strains, and forces induced in structures or components by loads that do not create substantial inertia or damping effects. Steady loadings and response conditions are envisaged, which means that the loads and responses of the structures are expected to fluctuate gently over time. Static structural analysis of fixed wing UAV is performed using Ansys. The loading applied in this analysis includes a pressure load obtained from CFD analysis of UAV. The complete methodology of performing static structural analysis of UAV is described as following:

3.6.1 Geometry

3D model of UAV was designed using CAD software named as SOLIDWORKS and geometry was imported in Ansys structural to perform static structural analysis. The geometry of the model is shown in the figure below:
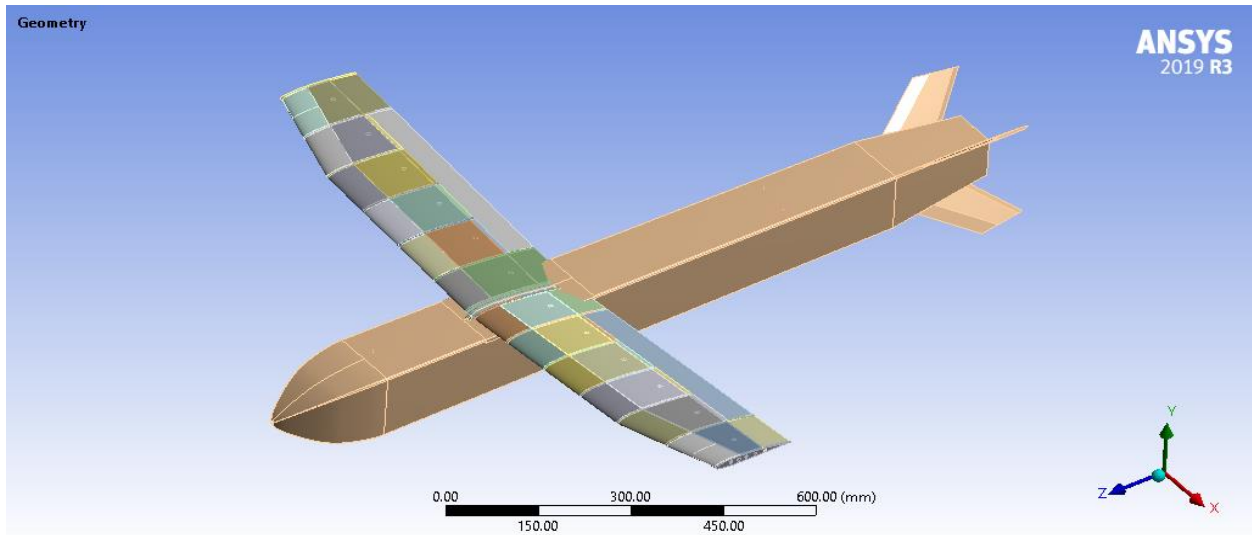
Figure 31 Geometry of UAV

3.6.2 Materials

Three materials are used for structural analysis. Aluminum alloy, stainless steel, Carbon-Epoxy composite are used respectively to perform analysis on complete UAV frame with following related mechanical properties:

3.6.2.1   Aluminum alloy

Density	2770 kg/m^3
Young's Modulus	7.1e+10 Pa
Poisson's ratio	0.33
Yield strength	2.8e+08 Pa

Figure 32 Mechanical properties of aluminum alloy

3.6.2.2   *Stainless steel*

Density	7750 kg/m^3
Young's Modulus	1.93e+11 Pa
Poisson's ratio	0.31
Yield strength	2.07e+08 Pa

Table *6*. Mechanical properties of stainless steel

3.6.2.3   *Carbon-Epoxy*

Epoxy (EP) matrix, high strength carbon fiber unidirectional tape prepreg, quasi-isotropic laminate [0/+45/-45/90] s (unidirectional tape prepreg, fiber Vf:0.55-0.65, autoclave cure at 115-180°C, 6-7 bar) is used with following mechanical properties are:

Density	1565 kg/m^3
Young's Modulus	5.465e+10 Pa
Poisson's ratio	0.306
Yield strength	6.667e+08 Pa

Table7. Mechanical properties of carbon-epoxy composite

3.6.3 Meshing

3D computational meshing of complete UAV frame is carried out using tetrahedral and cubic elements. For the fuselage and internal frame, tetrahedral meshed elements are used with an element size of 3.5 mm while some parts of wings are meshed with cubic elements with same element size. Complete 3D mesh of the model is shown in figure below:
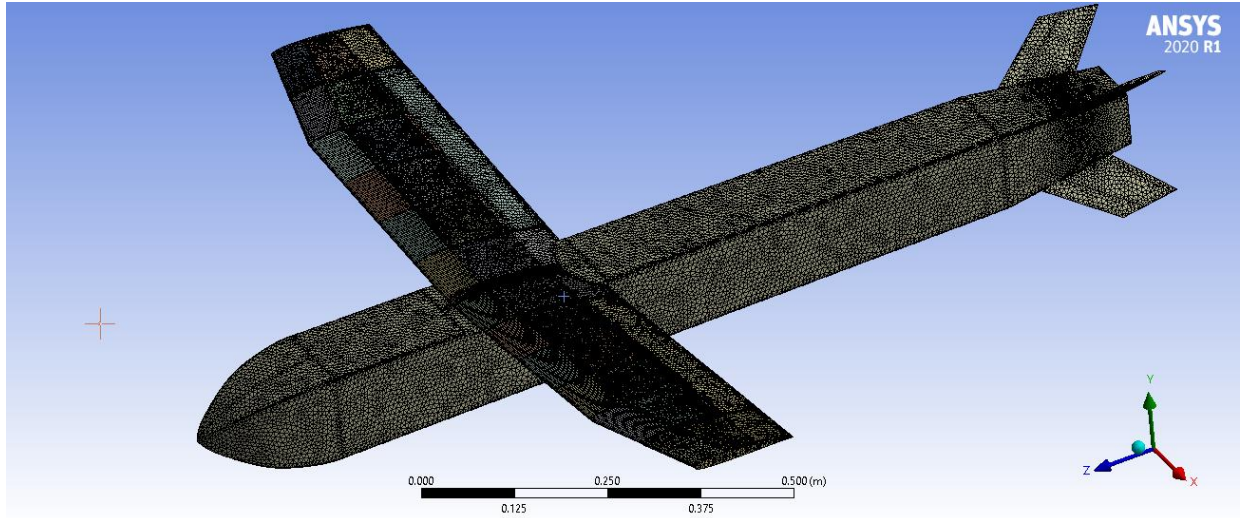
Figure 33 Computational Meshing of UAV
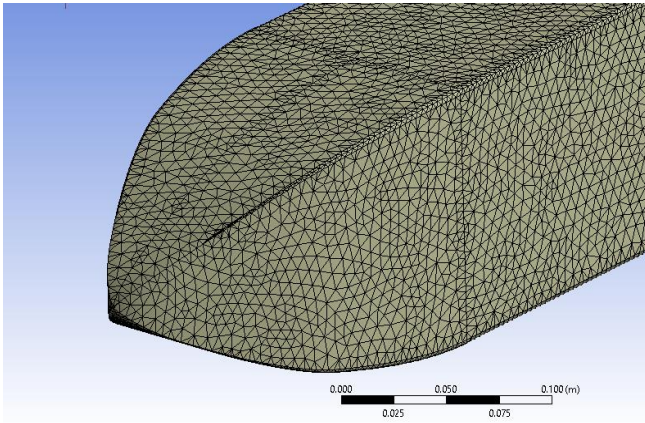
Figure 34 Tetrahedral elements for fuselage
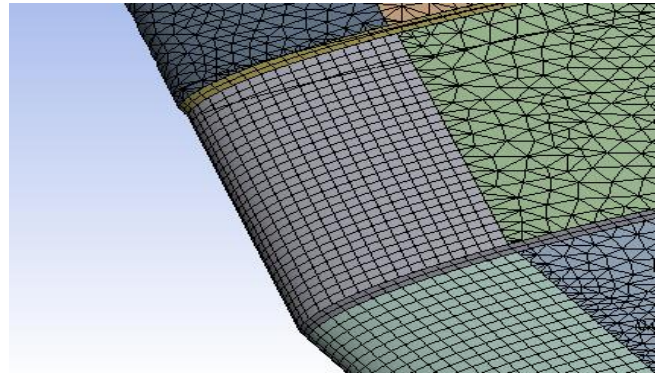
Figure 35 Tetrahedral and cubic elements for wings

3.6.4 Boundary Conditions

The model is analyzed as cantilever beam structure where wings are fixed to the fuselage with fixed support constraint and pressure (static pressure) load is applied on the surface of wings of UAV, obtained from aerodynamic analysis (CFD), to see the effect of this load on the UAV. The average static pressure value obtained from CFD is 21600 Pa. The boundary conditions on UAV for the analysis are shown in figure below:

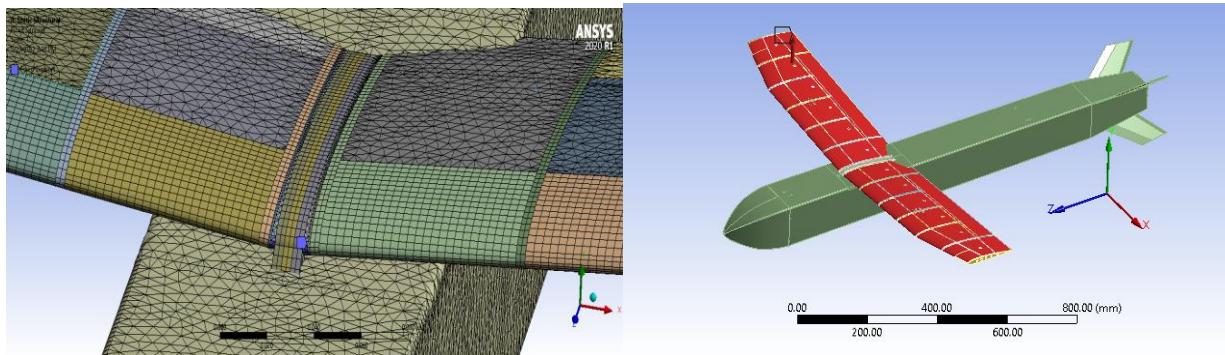**Figure 36 (a) Wings fixed to the fuselage.   (b) Applied pressure load.**

The results for deformation and stresses are obtained after running the solution. These results are shown in chapter 4.

3.7   Prototype Manufacturing Plan

A scaled model was manufactured using a variety of materials that are included in bill of materials table shown below. The manufacturing plan involved the welding of four stainless steel pipes of 1m length that were hollow from inside. We drilled the holes of 9mm thickness and passed 13 inches mild steel rods through them and welded them to reinforce our design. The interior fuselage was completed by spot welding at each joint. After this we cut the stainless-steel bars of 10mm thickness using plasma cutting technology and made our desired airfoil shapes. The material reduction on rods was carried out using EDM techniques. The holes 8mm were drilled using EDM machines as well. After this, we passed steel rods from the holes and welded to make the joints strong. At the end, we used aluminum sheets to cover our prototype. And we used rivets to join it

to the surface of our prototype. The tail was manufactured using mild-steel and it was covered using aluminum sheets and we got our final prototype weighing 28kg.

Materials and Cost of Manufacturing

Materials	Cost (Rs.)
Stainless steel (grade 19) pipes	12,000
Stainless steel (grade 17) pipes	8,000
Aluminum sheet (2.5 mm)	5500
Mild steel rods	3500
Rivets	700
Welding rods	2000
Stainless steel bars (10 mm) (x2)	15500
Drill Bit	4500
Plasma Cutting service	4000
EDM Drill Bit (Cadmium)	11000
Total Amount	66,700

4 Chapter 4: RESULTS AND DISCUSSION

4.1 CFD results

4.1.1 Pressure contours:

The UAV is simulated at both sea-level and 6000m altitude, because of which it experienced different magnitudes of pressures at the two conditions. Since the air is much lighter (low density) at higher altitudes, it experiences less pressure as shown by the contours below:
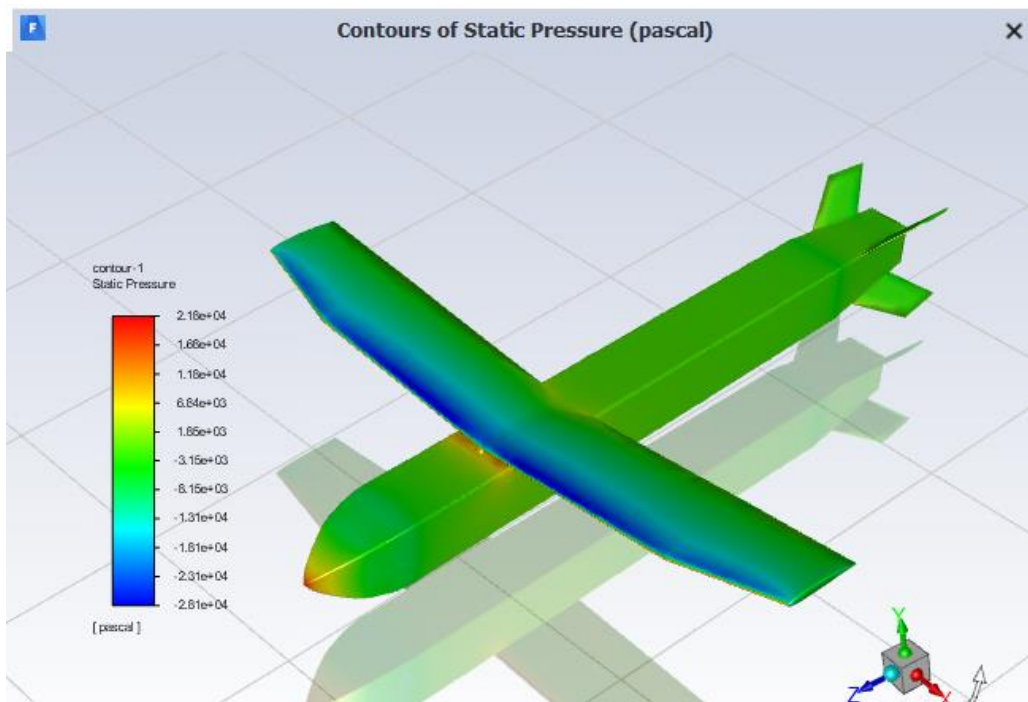
Figure 37 Pressure contours at sea-level (low altitudes)
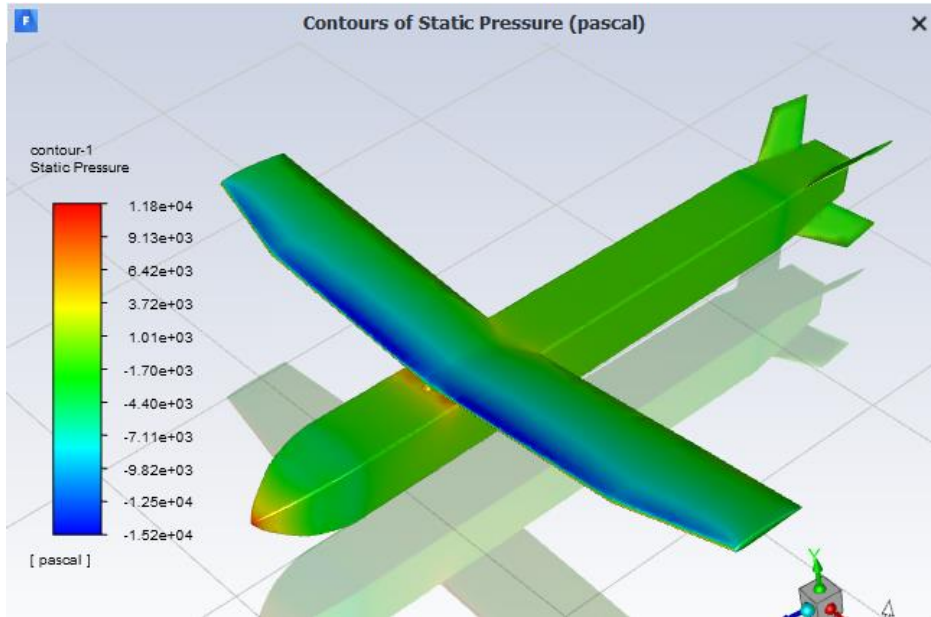
Figure 38 Pressure contour at 6000m (high altitudes)

4.1.2 Velocity contours:

The velocity contours for the uav as well as the airfoil for 0 and 5-degree angles of attack are shown in figures below. The air first stops at the front of body (stagnation point), then accelerates with achieving maximum speed (around 260 ms^{-1}) at the portion after the leading edge of airfoil.
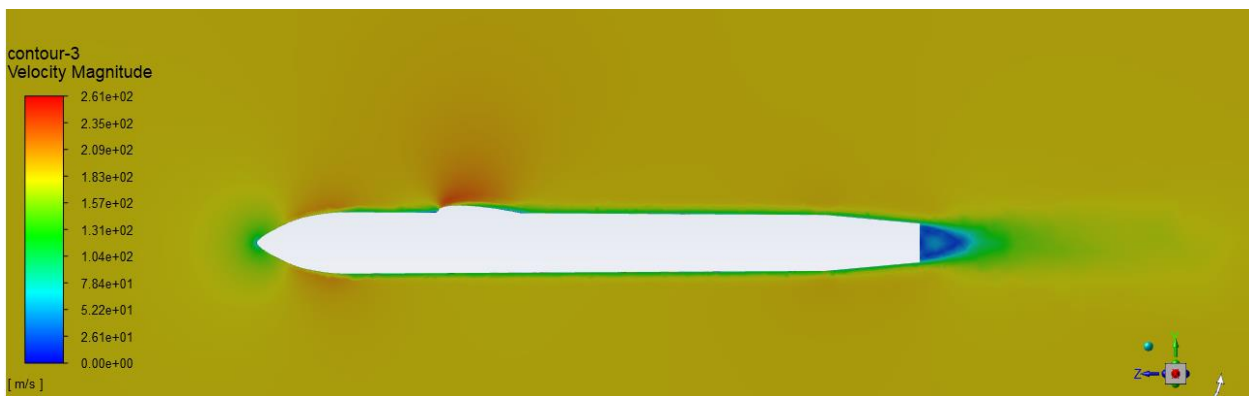
Figure 39 Velocity contours around the uav
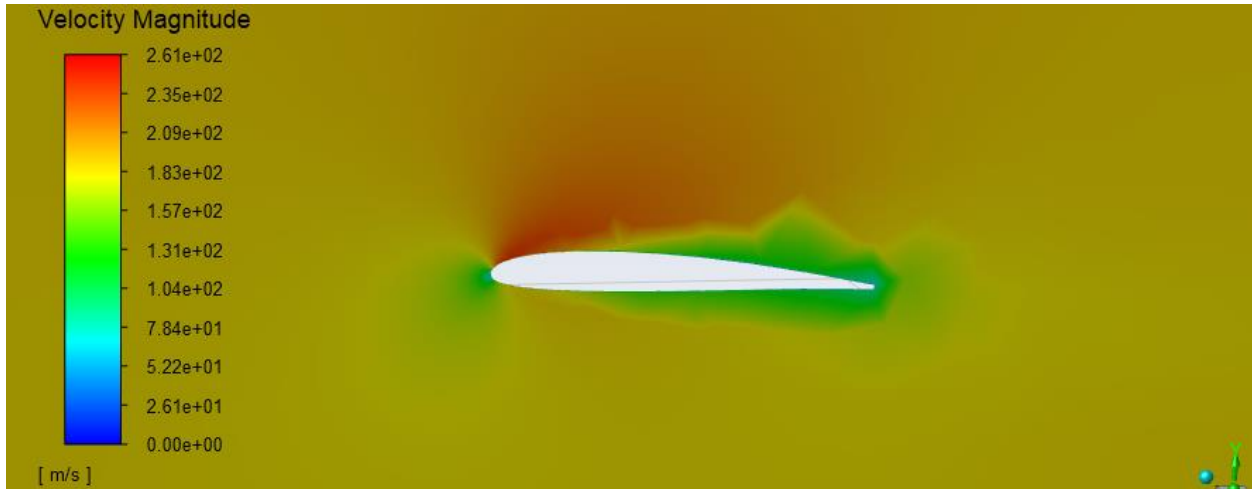
Figure 40 Velocity contours for airfoil at 0-degree AoA
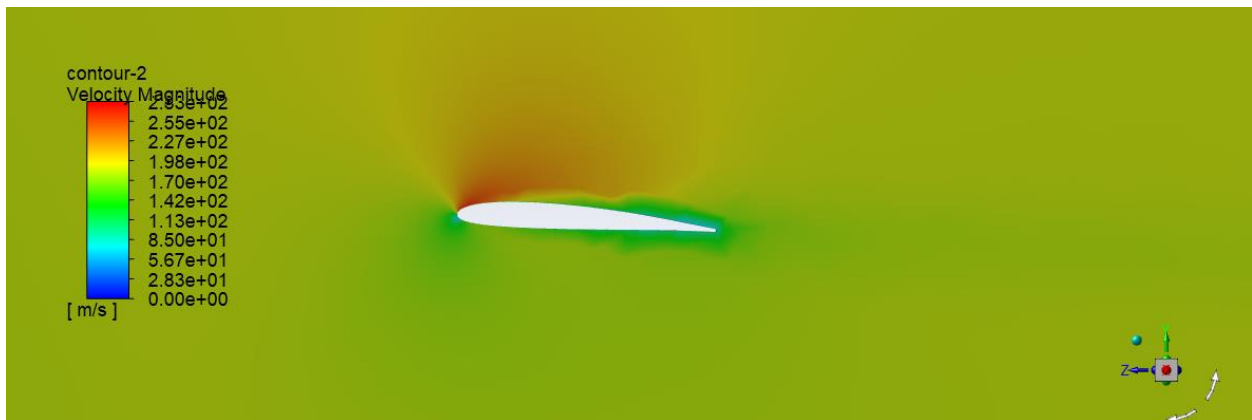
Figure 41 Velocity contours for airfoil at 5-degree AoA

4.1.3 Drag coefficient (C_d):

The plot for cd for both 0 and 5-degree AoA is displayed in figures below. At higher AoA, the value for cd increases (a compromise for higher lift as well as higher Cl/Cd ratios)
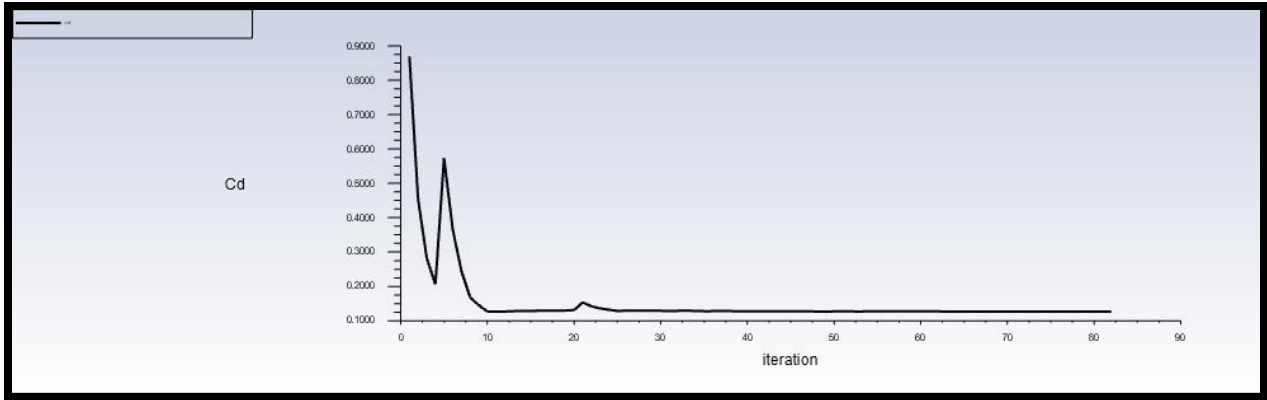
Figure 42 Cd at 0-degree AoA (Cd=0.1266)
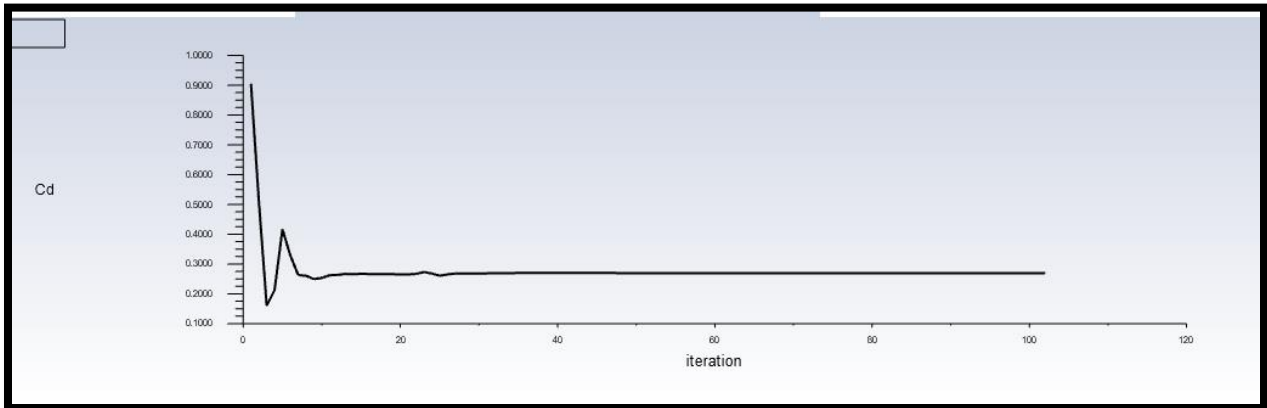
Figure 43 Cd at 5-degree AoA (Cd=0.269)

4.1.4 Lift coefficient (C_L):

The plot for C_L for both 0 and 5-degree AoA is displayed in the figures below. At higher AoA, the value for C_L increases until decreasing suddenly at very high AoA (stall).
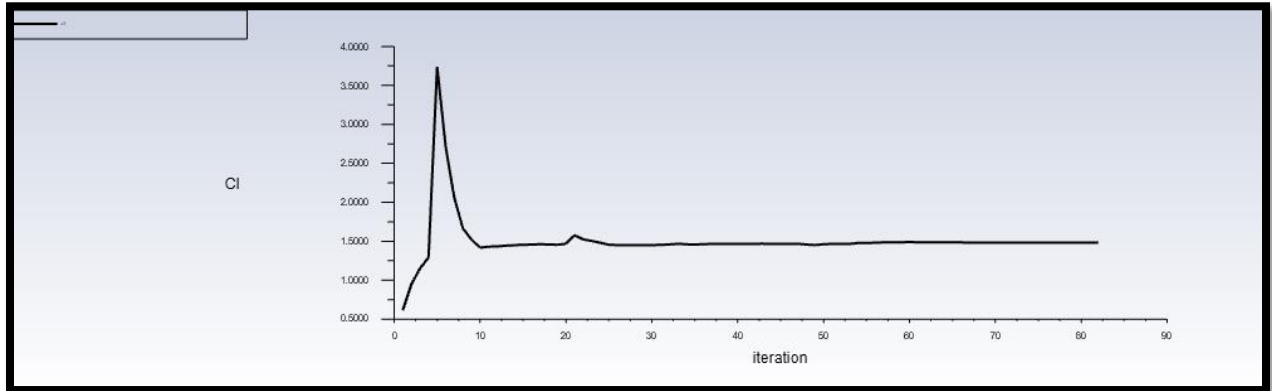
Figure 44 CL at 0-degree AoA (CL=1.48)
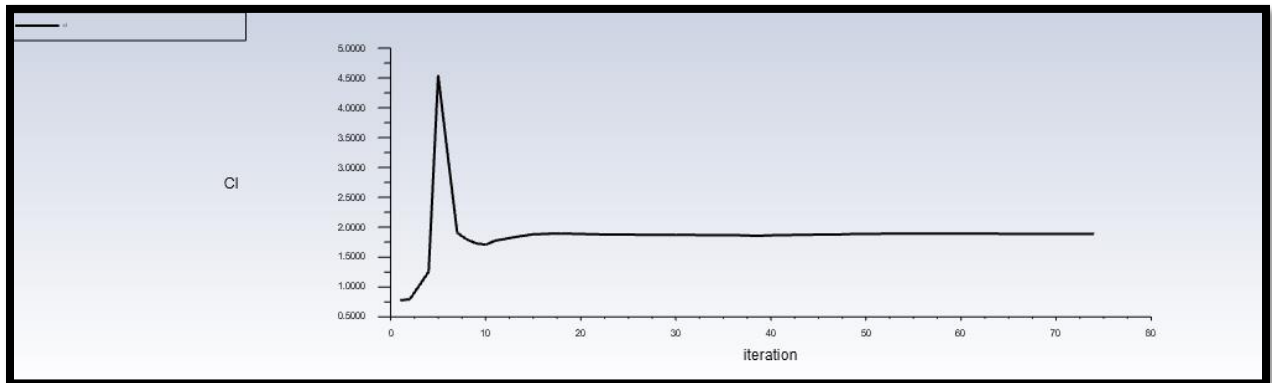
Figure 45 CL at 5-degree AoA (CL=2.159)

4.1.5 Pressure coefficient (C_P):

Pressure coefficients are important since the area between the lines on the distribution is a direct measure of lift generated. The C_p distribution for the UAV as well the contour around the airfoil is displayed in figures below:
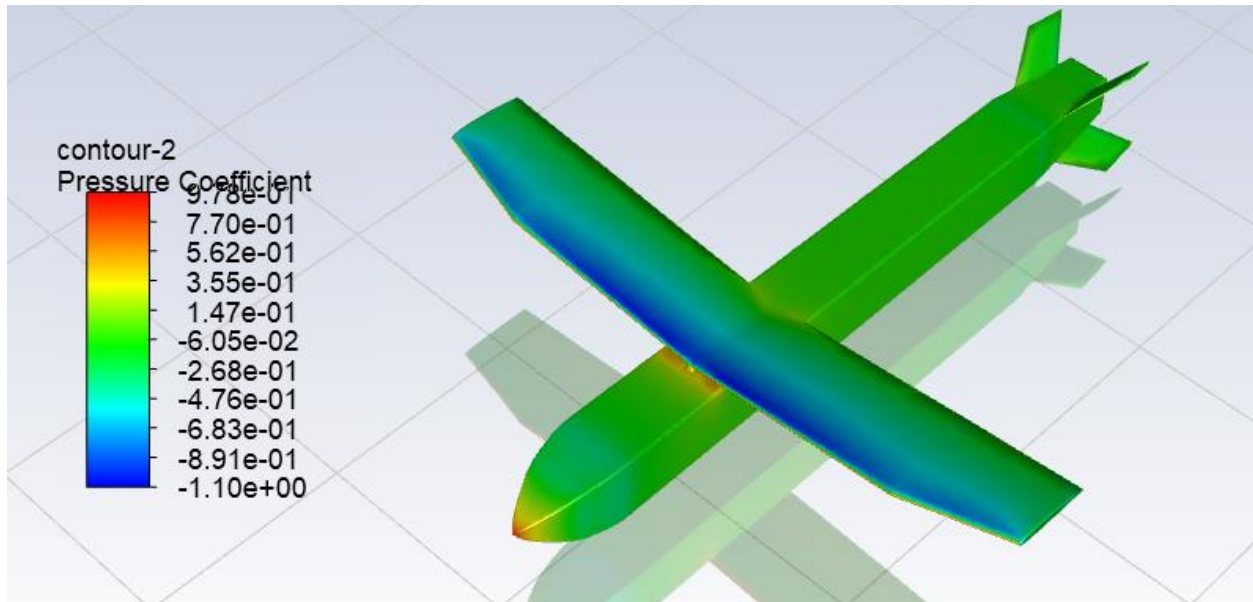
Figure 46 Cp distribution around the UAV body
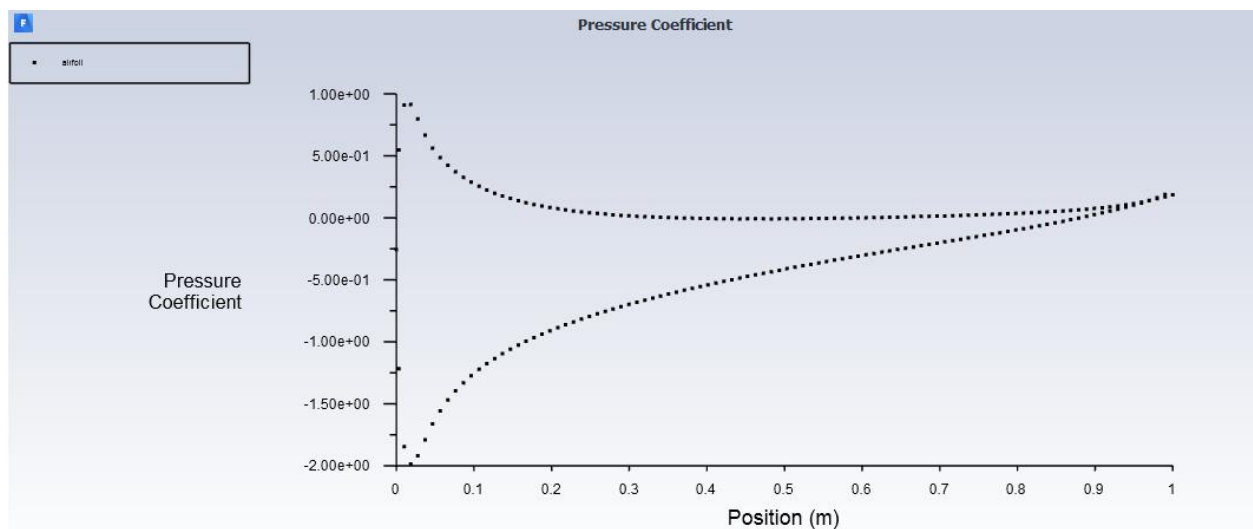
Figure 47 Cp around airfoil section

4.2   Mesh Independence study:

A mesh independence study is also performed using coarse, medium, and fine meshes in order to ensure that the results do not show significant variations depending on the mesh size. The results from study are summarized in the table below:

Variables	Coarse	Medium	Diff.	Fine	Diff.
Elements	1.5M	2M	-	3M	-
Drag coefficient	0.269	0.264	1.86%	0.266	0.75%
Lift coefficient	2.152	2.06	4.28%	2.09	1.44%

Table 8 Mesh independence study

4.3   Validation of CFD results:

Analytical calculations are done using MATLAB (shown in Appendix II). The comparison between the two calculations is summarized in table below:

Variables	Theoretical value	Result from CFD	Difference
Drag coefficient	0.273	0.269	1.46%
Lift coefficient	2.2679	2.159	4.89%

Table 9 Results validation

Since the CFD results are very close to the analytical calculations (within 5% error), we can confidently say that the analysis is correct.

4.4   FEA Results

The results for deformation and stresses are shown in figures below:

4.4.1 Deformation results

Deformation in different components of UAV with different materials are shown in figures below:
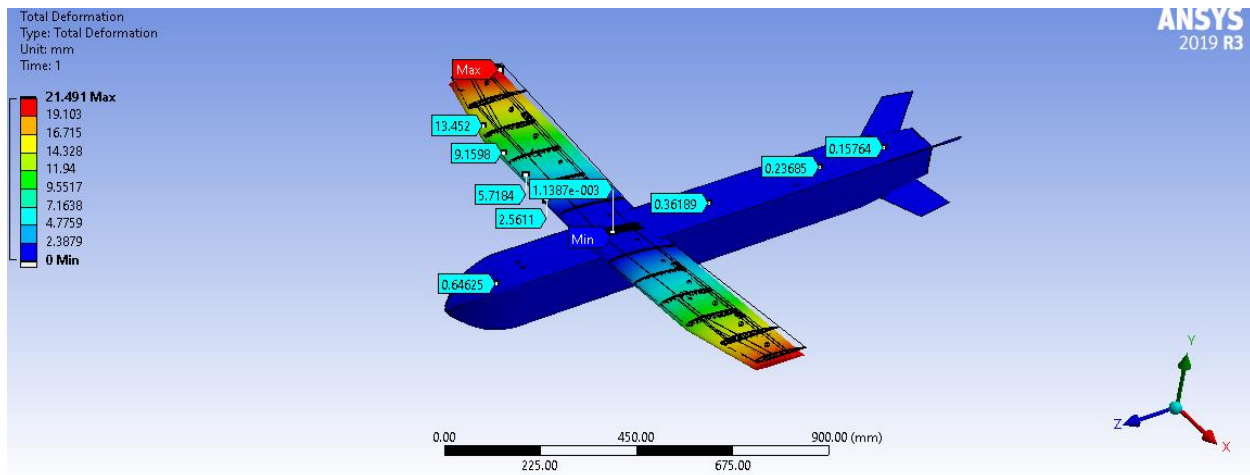
Figure 48 Deformation at different locations in UAV (Aluminum alloy)
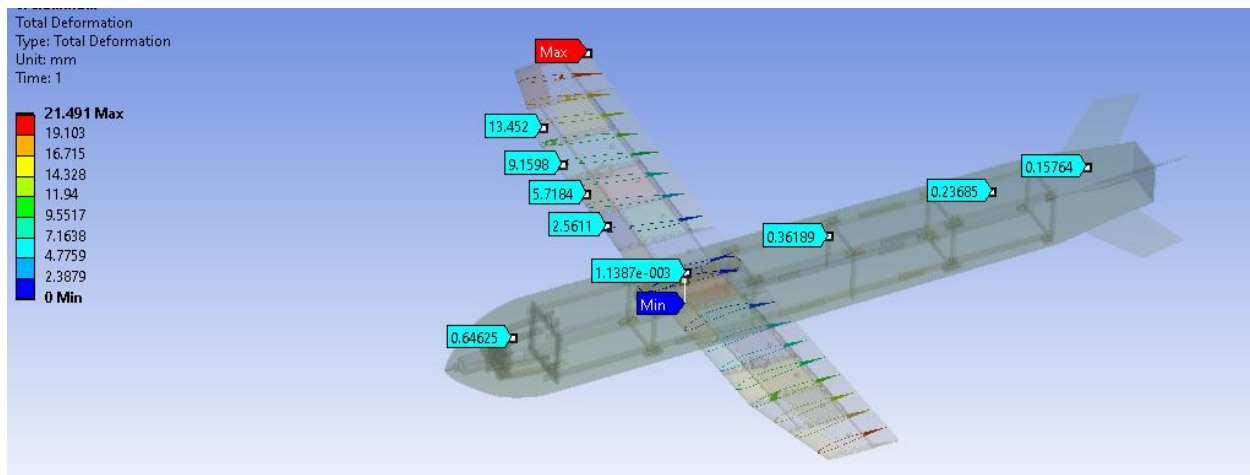
Figure 49 Deformations in the interior structure (aluminum alloy)
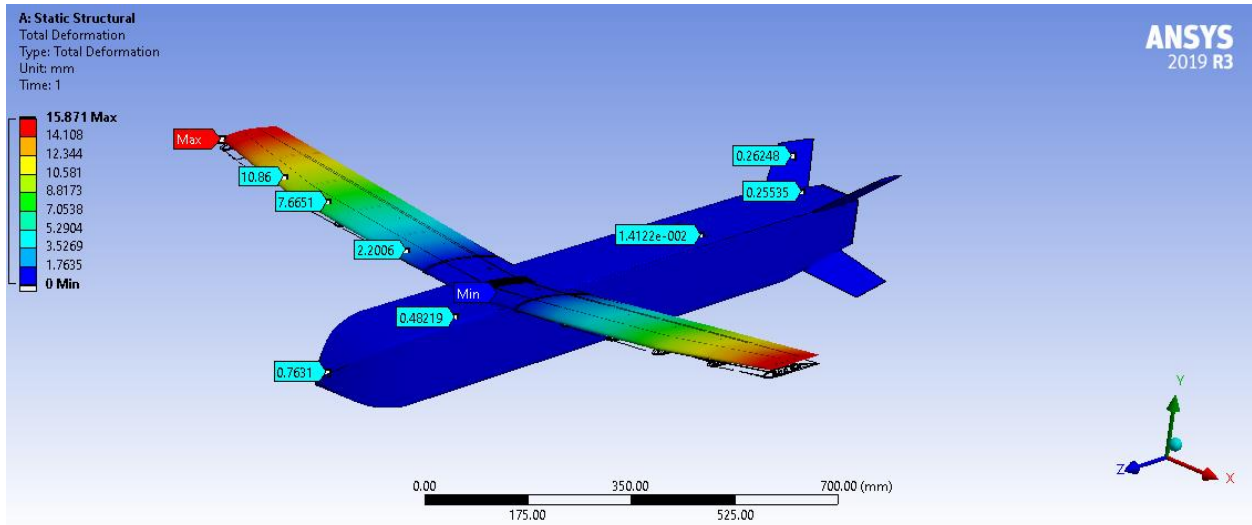
Figure 50 Deformation at different locations in UAV (Stainless steel)
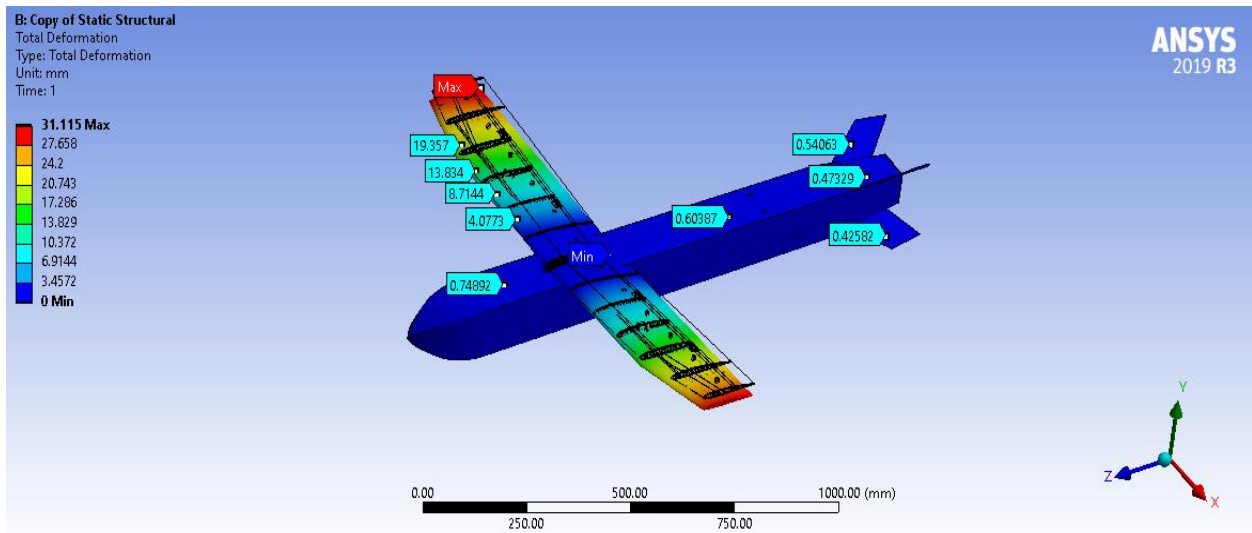
Figure 51 Deformation at different locations in UAV (Carbon-Epoxy composite)

4.4.2 Stress Results

The key stress results in different components of the structure with different materials are shown in figures below:
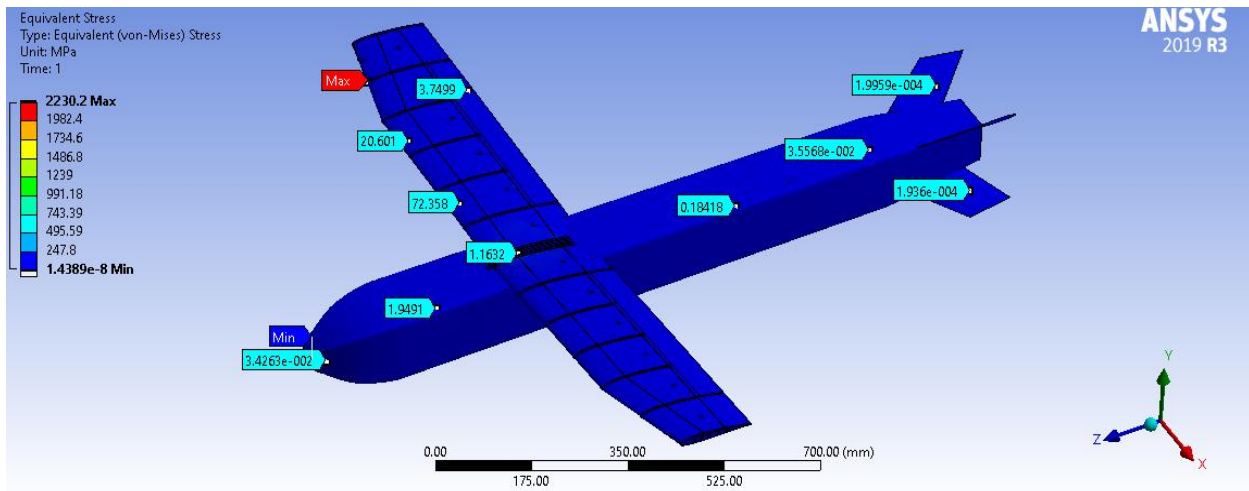
Figure 52 Equivalent Von-Misses stress at different locations (Aluminum alloy)
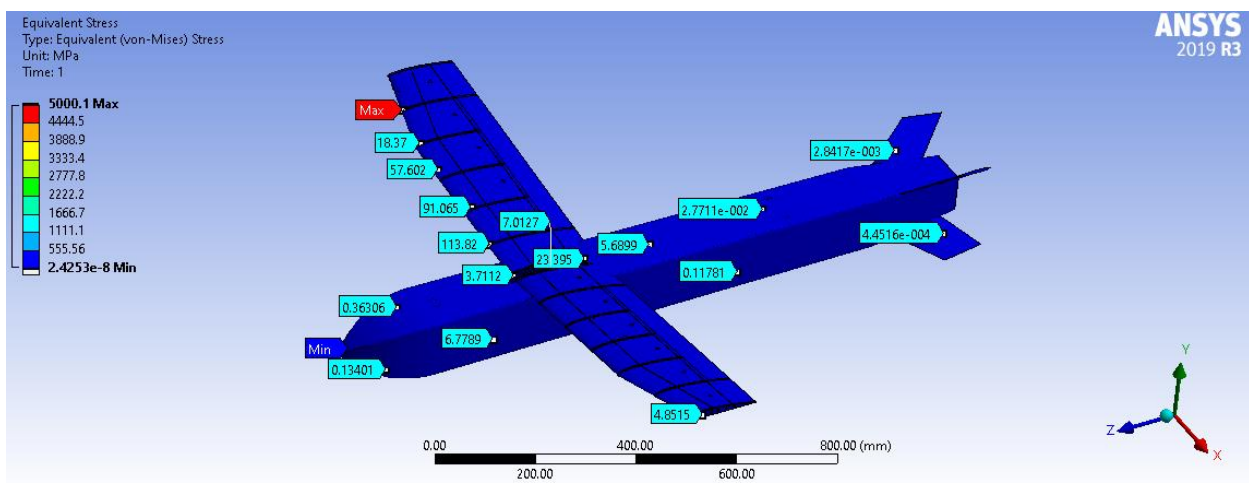
Figure 53 Equivalent Von-Misses stress at different locations (Stainless steel)
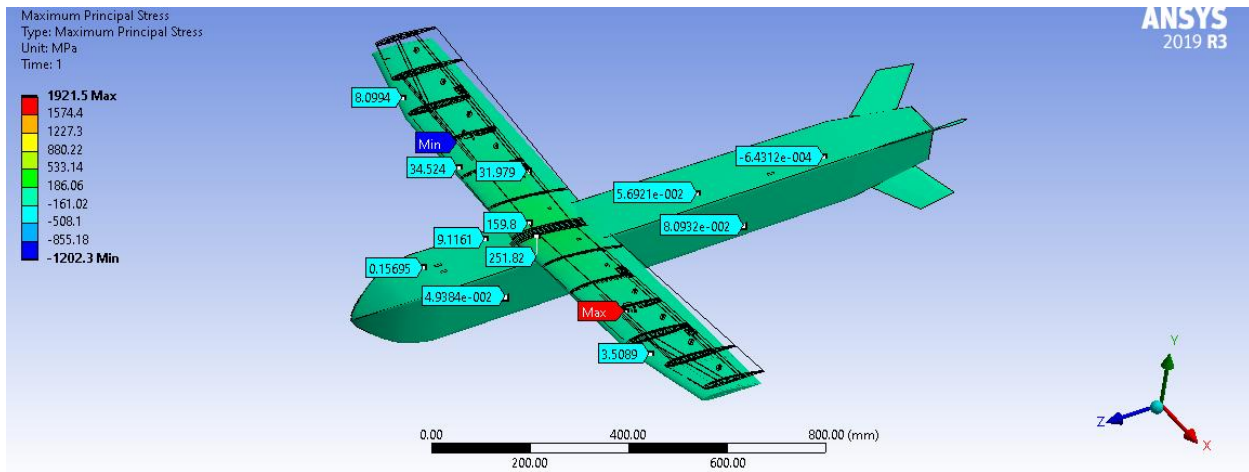
Figure 54 Maximum Principal Stress (Carbon-epoxy composite)

4.4.2.1 Region of maximum stresses
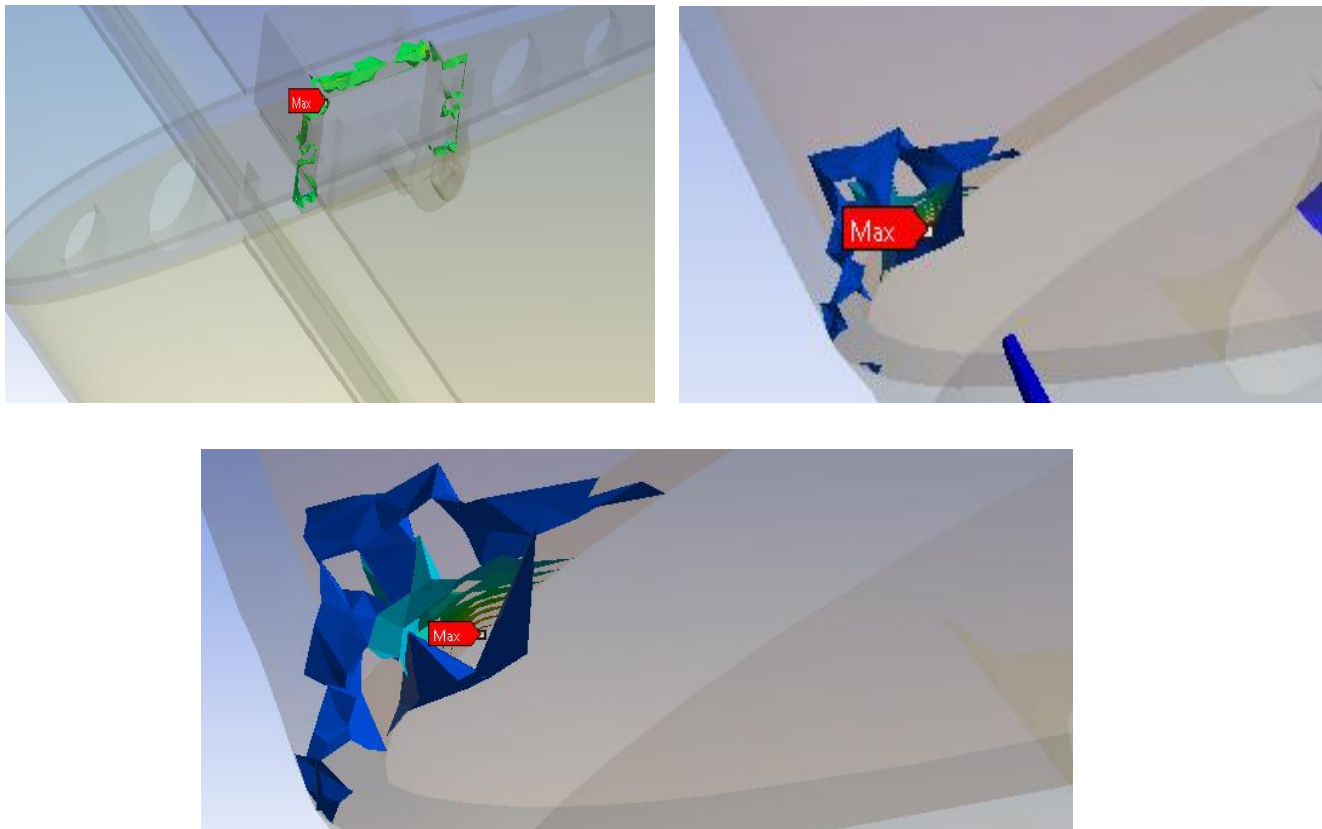
Figure 55 Maximum stress region. (a) 1921 MPa (Carbon-epoxy composite). (b) 5000 MPa (Stainless steel). (c) 2230 MPa (Aluminum alloy)

4.4.3 Factor of Safety

The factor of safety for our design is calculated by the Ansys and the maximum value comes out to be 5 (blue region) and minimum value is 1.5 (red region).
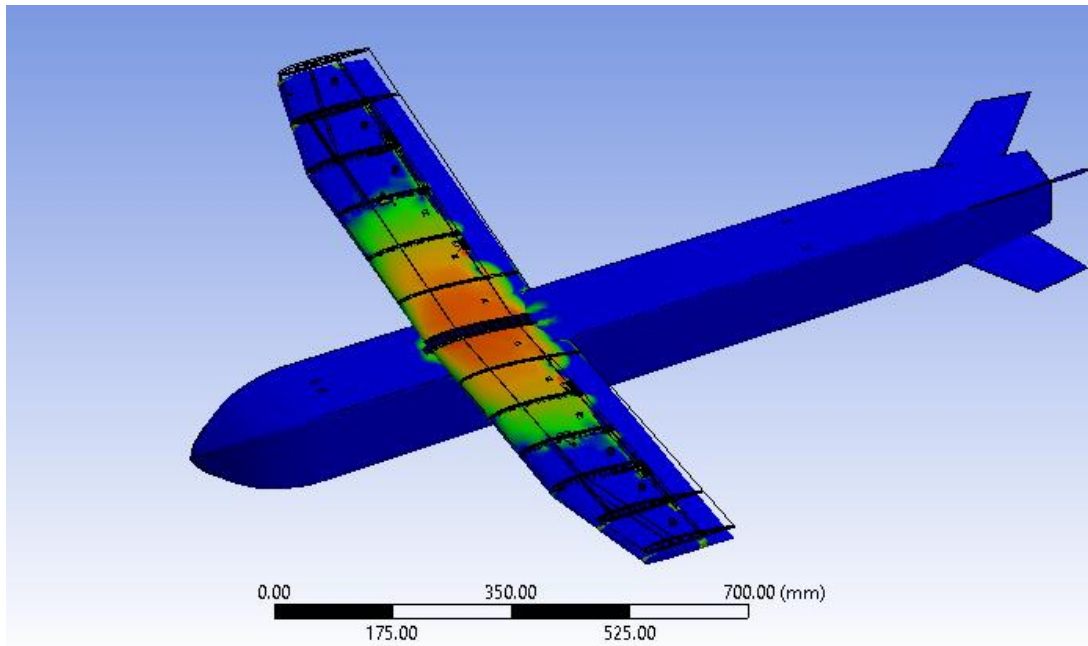
Figure 56 Factor of safety

4.5   FEA Results discussion

As the wings are fixed to the fuselage, it can be seen that maximum deformation occurs at the wing tip and decreases towards the root of the wing attached to the fuselage. The maximum and minimum deformations in case of aluminum are 21.49 mm and 0 mm. The wing deflects in the downward direction. The maximum and minimum deformations in case of stainless steel are 15.871 mm and 0 mm. The deflection of wing is in the upward direction. The maximum and minimum deformations in case of composite material are 31.12 mm and 0 mm and wing shows deflection in downward direction from its original position. The fuselage (reinforcements) shows minimum deflection throughout its structure.

Equivalent (von-misses) stresses contours are represented in above figures for aluminum alloy and stainless-steel materials showing the stress values at different locations in the structure. The rib at the tapered end of the wing shows the maximum stress concentration while minimum stress occurs

at the nose of the UAV as shown in above figures. Von-misses stress results are used to compare the equivalent stress to the yield stress of the material to judge the failure condition of the material (structure). Maximum and minimum stress values are 2230.2 MPa in rib region of wing and 1.438e-8 MPa in nose region of UAV respectively when the analysis is performed using aluminum alloy. The average stress value is 14.064 MPa in the structure. The overall stress generated in the structure is of very small magnitude. In the similar fashion, Maximum and minimum stress values are 5000.1 MPa in rib region of wing and 2.4253e-8 MPa in nose region of UAV respectively when the analysis is performed using aluminum alloy. The average stress value is 28.565 MPa in the structure.

The analysis performed with carbon-epoxy composite shows the principal stress values at different regions in the structure. The maximum and minimum values are 1921.5 MPa and -1202.3 MPa respectively. The average value of principal stress 8.4922 MPa. The stress result values with composite material are quite realistic and of very small values in magnitudes as compared to other two materials. The high strength to weight ratio of carbon-epoxy UD prepreg composite make it useful to use in fuselage and wing structure of UAV.

5 Chapter 5: CONCLUSION AND RECOMMENDATIONS

The CFD analysis of our UAV was successfully performed using Ansys fluent. The simulation was setup with appropriate boundary conditions, after proper meshing. Contours for static pressure, velocity as well as the pressure coefficient were plotted to analyze the fluid flow around the UAV. The final design has a Cd of 0.273 along with a lift coefficient of 2.769 operating at 5-degree AoA. The results were also validated through the analytical calculations, and they were within the 5% accuracy. The CFD results were then imported to perform FEA analysis using one-way FSI. Through this analysis, we managed to confidently design the fixed-wing UAV as per the industry specifications.

For the described boundary conditions, it can be concluded that maximum deformation value which occurs at the tip of the wing is least for stainless steel having a value of 15.87 mm which is smaller as compared to other two materials used. Therefore wings (with ribs and spars) of UAV can be fabricated with stainless steel. This deformation can also be reduced by thickening some surfaces of wing structure. The finite element model is assumed to be a model of cantilever beam which shows the significant amount of deflection at the free end and minimum value of deflection at the fixed end.

From the stress results, it is evident that maximum stress occurs in one of the ribs of the wing where equivalent (von-misses) stress result exceeds the yield strength of both materials i.e., aluminum alloy and stainless steel due to which the structure (rib of wing) fails from that region. Therefore, it is highly recommended to use titanium alloy in ribs of wings to prevent such failure from high pressure loads. The blue colored counters show that overall stress generated in the structure is very low as compared to the yield strength of both the ductile materials used for analysis. Fuselage can be fabricated with any of the above-mentioned materials since the stresses generated in the fuselage are of very small values but to have high strength to weight ratio for the fuselage structure, carbon-epoxy UD prepreg composite (quasi-isotropic laminate [0/+45/-45/90] s) is highly recommended as it gives extra strength to the structure and avoid failure at high loads.

As technology is improving, to adapt with it and make UAVs faster, accurate and better some steps can be taken. We studied deeply the results obtained from FEA and CFD and by using topology optimization we can improve our design and reduce our cost by huge scale. Most UAV designers try to keep a vehicle's drag as low as possible to optimize endurance. While low drag is desired in flight, it might present difficulties during landing. Because operators require extended final approaches to lower a UAV's height during a circuit, this is the case. In addition, shallow glideslopes make it difficult for UAVs to land in obstructed areas (such as wooded areas or fields ordered by trees). To remedy this, UAV design teams incorporate an effective method of steepening the glideslope of the UAV, such as with spoilers or flaps. Operators can conduct belly landings in tight spaces with good approach control. Also, we can use OpenCV and python to do image scanning and matching targets which will be better than simple coordinate system. Endurance in UAV holds a lot of importance. When all design team's efforts are focused on aerodynamics, endurance, payload, speed, weight, and drag, many of them miss the point. UAVs are built with a specific function in mind. Therefore, design teams should priorities the value and operation of the payload over any other design concern. The payload's carrying capacity is important; but the payload's position is even more important. The best locations depend on the payload type. Still-picture 'cameras are quite straightforward to put in the middle of the UAV. Design teams should ensure that the camera is easily accessible and that enough shielding is provided to prevent damage during landing.

REFERENCES

[1] Classification of unmanned aerial vehicle (UAV). Retrieved from: https://www.academia.edu/download/29666442/group9.pdf

[2] How a quadcopter works (2012). Retrieved from:

http://ffden-2.phys.uaf.edu/webproj/212_spring_2014/Clay_Allen/clay_allen/works.html

[3] Aircraft fuselage parts and types : truss and skin stressed | Monocoque Structure (2021). Retrieved from:

https://www.youtube.com/watch?v=pmZga5ah2jg

[4] Major Aircraft Components Including, Fuselage and empennage by will Liebhaber (2016). Retrieved from:

https://www.youtube.com/watch?v=eYRRTJsKbhU&t=307s

[5] Aircraft Wing terms (2014) Retrieved from: http://sahil34935.blogspot.com/2013/02/aircraft-wing-terms.html

[6] Flight Mechanic. Retrieved from: https://www.flight-mechanic.com/empennage/

[7] Aircraft wing structure design project (2021) by Huskey Engineering. Retrieved from:

Aircraft Wing Structure Design Project - YouTube

[8] UAV Design and Manufacture. Retrieved from: http://citeseerx.ist.psu.edu/viewdoc/download?doi=10.1.1.457.379&rep=rep1&type=pdf

[9] How To Keep the Courant Number Below 1? Retrieved from: https://www.simscale.com/knowledge-base/what-is-a-courant-number/

[10] Real External Flows. Retrieved from:

https://courses.ansys.com/index.php/courses/real-external-flows/

[11] What is y+ (yplus). Retrieved from:

https://www.simscale.com/forum/t/what-is-y-yplus/82394

Appendix I: Design Calculations

Design Calculations (MATLAB Code):

```
clc

clear all

H    = 6000;        %% altitude (m)
W_t  = 6370;         %% total weight (N)
W_f  = 2940;         %% fuel weight  (N)
W_e  = 3430;          %% empty weight (N)
V    = 190;          %% velocity   (m/s)
S    = 0.234;        %% surface area (m2)
M    = 0.6;          %% mach number
L_D  = 11;            %% lift to drag ratio
Cd_o = 0.016;         %% skin friction drag
K    = 0.05;         %% constant
rho  = 0.665;         %% density
W_dot= 12 * (9.8/60);  %% specific fuel consumption (kg/min)
```

thrust and Lift required %%

```
C_L  =  ((2*W_t)/(rho*(V^2)*S))


C_D  =  Cd_o + (K*(C_L^2))


T  =  (0.5)*(rho)*(V^2)*(S)*(C_D)


L = (0.5)*(rho)*(V^2)*(S)*(C_L)


%%%%%%%%%%%%%%%%%%%%%%%%%%%%%%%%%%%%%%%%%%%%%%%%%%%%%%%%%%%%%%%%
%%%%
```

C_L =

2.2679

C_D =

0.2732

T =

767.2677

L =

6370

Range %%

```
Ct = (W_dot)/T;

R  = (2/Ct)*(sqrt(2/(rho*S)))*(sqrt(C_L)/C_D)*(sqrt(W_t)-sqrt(W_e));

R_km = R/1000

%%%%%%%%%%%%%%%%%%%%%%%%%%%%%%%%%%%%%%%%%%%%%%%%%%%%%%%%%%%%%%%%%%%%%%%%%%%%%%
%%%%
```

R_km =

328.7578

time/ ENDURANCE %%

```
E = (1/Ct)*(L_D)*log(W_t/W_e);

E_min = E/60

%%%%%%%%%%%%%%%%%%%%%%%%%%%%%%%%%%%%%%%%%%%%%%%%%%%%%%%%%%%%%%
%%%%%
```

E_min =

   44.4274

Appendix II: Solidworks Drawings

6 5 4 3 2 1

1.50
R17.50
R8.57
R3.00
95.00
38.00
110.00

R4.00 76.30 196.00 R1.50 15.00
3.00
46.00 3.32 1110.00
1201.90 15.00
196.00

Ø17.13
64.00
46.00 17.00
52.83 76.30
R1.50

R11.40
15.00
6.64

90.00 400.00

1201.90

110.00

D C B A

	NAME	SIGNATURE	DATE			
DRAWN						
CHK'D						
APPV'D						
MFG						
Q.A						

UNLESS OTHERWISE SPECIFIED:
DIMENSIONS ARE IN MILLIMETERS
SURFACE FINISH:
TOLERANCES: 0.0001
LINEAR:
ANGULAR:

FINISH:

DEBURR AND BREAK SHARP EDGES

DO NOT SCALE DRAWING REVISION

TITLE:
Fuselage

MATERIAL:
Stainless Steel

DWG NO.
Fuselage A4

WEIGHT: SCALE:1:12 SHEET 1 OF 1

Final Assembly

UNLESS OTHERWISE SPECIFIED: DIMENSIONS ARE IN MILLIMETERS SURFACE FINISH: TOLERANCES: LINEAR: 0.0001 ANGULAR:	FINISH:			DEBURR AND BREAK SHARP EDGES	DO NOT SCALE DRAWING	REVISION	

	NAME	SIGNATURE	DATE				
DRAWN					TITLE:		
CHK'D					Final Assembly		
APPV'D							
MFG							
Q.A				MATERIAL: Stainless steel/ aluminum	DWG NO. Final Assembly		A4
				WEIGHT:	SCALE:1:24	SHEET 1 OF 1	

Appendix iii: Air properties at different altitude

Geo potential Altitude above Sea Level - h - (m)	Temperature - t - (^oC)	Acceleration of Gravity - g - (m/s^2)	Absolute Pressure - p - (10^4 N/m^2)	Density - ρ - (10^{-1} kg/m^3)	Dynamic Viscosity - μ - (10^{-5} N.s/m^2)
-1000	21.50	9.810	11.39	13.47	1.821
0	15.00	9.807	10.13	12.25	1.789
1000	8.50	9.804	8.988	11.12	1.758
2000	2.00	9.801	7.950	10.07	1.726
3000	-4.49	9.797	7.012	9.093	1.694
4000	-10.98	9.794	6.166	8.194	1.661
5000	-17.47	9.791	5.405	7.364	1.628
6000	-23.96	9.788	4.722	6.601	1.595
7000	-30.45	9.785	4.111	5.900	1.561
8000	-36.94	9.782	3.565	5.258	1.527
9000	-43.42	9.779	3.080	4.671	1.493
10000	-49.90	9.776	2.650	4.135	1.458
15000	-56.50	9.761	1.211	1.948	1.422
20000	-56.50	9.745	0.5529	0.8891	1.422
25000	-51.60	9.730	0.2549	0.4008	1.448
30000	-46.64	9.715	0.1197	0.1841	1.475
40000	-22.80	9.684	0.0287	0.03996	1.601
50000	-25	9.654	0.007978	0.01027	1.704
60000	-26.13	9.624	0.002196	0.003097	1.584
70000	-53.57	9.594	0.00052	0.0008283	1.438
80000	-74.51	9.564	0.00011	0.0001846	1.321